



UNIVERSITÀ
DEGLI STUDI
DI PADOVA



UNIVERSITÀ DEGLI STUDI DI PADOVA
DIPARTIMENTO DI INGEGNERIA DELL'INFORMAZIONE

CORSO DI LAUREA MAGISTRALE IN
BIOINGEGNERIA

**“Development of a 3D Culture Platform
for Multiple Myeloma Tumor Cells”**

Relatrice:

Prof.ssa Monica Dettin

Correlatore:

Prof. José Luís Gómez Ribelles

Laureanda:
Ludovica Rossi

ANNO ACCADEMICO 2023 – 2024

Data di laurea 16/04/2024

Abstract

The aim of this work is to contribute to the development of a 3D culture platform for Multiple Myeloma tumor cells in order to enable practical testing of antitumoral drugs. To achieve this, it is essential to replicate *in vitro* the interactions that Multiple Myeloma cells (MMCs) maintain *in vivo* with other cells of the tumor microenvironment, in particular mesenchymal stem cells (MSCs), and with proteins and polysaccharides of the bone marrow extracellular matrix. In order to do this, the cells must be cultured in a three-dimensional environment containing all the components of the real tumor microenvironment. At the Centre of Biomaterials and Tissue Engineering (CBIT), a model based on microgel is being developed. It consists in a suspension of microspheres in a liquid culture medium in which the MMCs will also be suspended. The culture conditions play a crucial role in preserving the viability and proliferation of these cells. However, due to the disease's heterogeneity, the behavior of each of the accessible MM cell lines can vary greatly.

In this work, with the help of microfluidics, we have made progress in the production and characterization of biomimetic microgels, which are based on alginate microspheres. The microspheres are approximately 150 μm in diameter and are covered in a multilayer of polyelectrolytes. The first layers of alginate and poly-L-lysine ensure the stability of the microsphere and are followed by a sequence of layers that present the polysaccharide of interest on the microsphere's surface. The three-dimensional environment of the cells consists of a mixture of microspheres functionalized with collagen, hyaluronic acid, heparin and chondroitin sulfate and suspended in Roswell Park Memorial Institute (RPMI) culture medium to which the cells are added.

The presence of these extracellular matrix components on the surface of the microspheres has been characterized. MMCs and supporting microspheres are deposited on conical agarose wells designed and produced by us. These wells are permeable to water and water-soluble substances. Co-culture with mesenchymal stem cells (MSCs) is performed by producing pellets of agglomerated cells with adherent microparticles for them. These pellets are added either inside or outside the wells to study the effect of direct or indirect contact between MSCs and MMCs. We first conducted a study on the effect of the frequency of changes of the liquid culture medium and other parameters of the culture protocol that probably determine the content in the medium of nutrients, as well as cytokines and other factors secreted by the cells. We tested the two most common glucose concentrations (2 g/L and 4.5 g/L) and found that changing the medium with the lowest concentration of glucose completely every two days yielded the best results.

Afterward, we tried to test the viability of the MM1.S cell line on the platform. Previous results of the response of cells from the RPMI8226 line were available, showing that the microgel favored cell proliferation and that there was little difference between direct and indirect co-culture. Very different behavior was found in the cells of MM1.S line compared to those of RPMI8226 line in terms of much lower proliferation both when cultured in the 3D environment created by the microgel and when cultured in suspension in the absence of microspheres. Finally, cell viability studies were carried out on the platform by subjecting the cells to treatment with Dexamethasone.

Keywords: 3D culture platform, multiple myeloma, disease modeling, tumor microenvironment, microgel, *in vitro* model, drug resistance.

Sommario

Lo scopo di questo lavoro è contribuire allo sviluppo di una piattaforma di coltura tridimensionale per le cellule tumorali di mieloma multiplo al fine di consentire test pratici di farmaci antitumorali. Per raggiungere questo obiettivo, è essenziale replicare *in vitro* le interazioni che le cellule di mieloma multiplo (MMCs) mantengono *in vivo* con altre cellule del microambiente tumorale, in particolare le cellule staminali mesenchimali (MSCs), e con proteine e polisaccaridi della matrice extracellulare del midollo osseo. Per fare ciò, le cellule devono essere coltivate in un ambiente tridimensionale che contiene tutti i componenti del reale microambiente tumorale. Al Centro di Biomateriali e Ingegneria Tissutale (CBIT), è in corso lo sviluppo di un modello basato su microgel. Consiste in una sospensione di microsfere in un terreno di coltura liquido in cui anche le MMCs saranno sospese. Le condizioni di coltura giocano un ruolo cruciale nel preservare la vitalità e la proliferazione di queste cellule. Tuttavia, a causa dell'eterogeneità della malattia, il comportamento di ciascuna delle linee cellulari di MM accessibili può variare notevolmente.

In questo lavoro, con l'aiuto della microfluidica, abbiamo fatto progressi nella produzione e nella caratterizzazione di microgel biomimetici, basati su microsfere di alginato. Le microsfere hanno un diametro di circa 150 μm e sono ricoperte da un multistrato di polielettroliti. I primi strati di alginato e poli-L-lisina assicurano la stabilità della microsfera e sono seguiti da una sequenza di strati che presentano il polisaccaride di interesse sulla superficie della microsfera. L'ambiente tridimensionale delle cellule è costituito da una miscela di microsfere funzionalizzate con collagene, acido ialuronico, eparina e solfato di condroitina e sospese nel terreno di coltura Roswell Park Memorial Institute (RPMI) a cui vengono aggiunte le cellule.

La presenza di questi componenti della matrice extracellulare sulla superficie delle microsfere è stata caratterizzata. MMCs e microsfere di supporto vengono depositate in pozzetti conici di agarosio progettati e prodotti da noi. Questi pozzetti sono permeabili all'acqua e alle sostanze idrosolubili. La co-coltura con cellule staminali mesenchimali (MSCs) viene eseguita producendo pellet di cellule agglomerate con microparticelle aderenti. Questi pellet vengono aggiunti sia all'interno che all'esterno dei pozzetti per studiare l'effetto del contatto diretto o indiretto tra MSCs e MMCs.

Abbiamo inizialmente condotto uno studio sull'effetto della frequenza dei cambi di terreno di coltura e di altri parametri del protocollo di coltura che probabilmente determinano il contenuto nel terreno di coltura di nutrienti, così come citochine e altri fattori secreti dalle cellule. Abbiamo testato le due concentrazioni di glucosio più comuni (2 g/L e 4,5 g/L) e abbiamo scoperto che cambiare completamente il terreno con la concentrazione più bassa di glucosio ogni due giorni ha prodotto i migliori risultati.

In seguito, abbiamo cercato di testare la vitalità della linea cellulare MM1.S sulla piattaforma. Erano disponibili risultati precedenti sulla risposta delle cellule della linea RPMI8226, che mostravano che il microgel favoriva la proliferazione cellulare e che c'era poca differenza tra la co-coltura diretta e quella indiretta. Un comportamento molto diverso è stato riscontrato nelle cellule della linea MM1.S rispetto a quelle della linea RPMI8226 in termini di proliferazione molto più bassa sia quando coltivate nell'ambiente tridimensionale creato dal microgel sia quando coltivate in sospensione in assenza di microsferi.

Infine, sono stati condotti studi sulla vitalità cellulare sulla piattaforma sottoponendo le cellule a trattamenti con Dexametasone.

Parole chiave: piattaforma di coltura tridimensionale, mieloma multiplo, modellazione della malattia, microambiente tumorale, microgel, modello *in vitro*, resistenza ai farmaci.

Acknowledgments

I would like to express my heartfelt appreciation to all those who have supported and contributed to the completion of my master's thesis. First and foremost, I am deeply thankful to Professor José Luís Gómez Ribelles and the entire CBIT team for their unwavering support, invaluable guidance, and insightful feedback throughout every stage of my research work.

I am also immensely grateful to Inmaculada García Briega, whose mentorship and encouragement have been invaluable throughout my journey. I am profoundly grateful for her teachings, patience, and unwavering belief in my abilities.

Additionally, I would like to express my gratitude to my supervisor, Professor Monica Dettin, who has been a great inspiration to me, sparked my passion for biomaterials and tissue engineering, and allowed me to take part in such a wonderful experience.

Index

| | |
|---|-----------|
| 1. Introduction | 15 |
| 1.1. Bone Marrow | 15 |
| 1.2. Hematopoiesis and Plasmatic Cells..... | 16 |
| 1.3. Bone Marrow Composition | 18 |
| 1.3.1. Cellular Component of Bone Marrow | 19 |
| 1.3.2. Bone Marrow Extracellular Matrix..... | 21 |
| 1.4. Multiple myeloma..... | 21 |
| 1.1. Multiple Myeloma Treatments | 22 |
| 1.1.1. Dexamethasone | 24 |
| 1.2. Tumor Microenvironment..... | 24 |
| 1.3. Drug Resistance in Multiple Myeloma | 24 |
| 1.3.1. Influence of the BM Microenvironment on Drug Resistance | 25 |
| 1.3.2. Interactions Between mPCs and ECM Components and their Effect on CAM-DR | 26 |
| 1.4. 2D and 3D Culture Systems | 28 |
| 1.4.1. Microgel..... | 30 |
| 1.5. 3D Multiple Myeloma Culture Platforms | 32 |
| 2. Aim of the study | 36 |
| 3. Materials and Methods | 39 |
| 3.1. Materials..... | 39 |
| 3.2. Microspheres' Production..... | 40 |
| 3.3. Microspheres' Functionalization | 41 |
| 3.3.1. Layer-by-layer of Poly-L-Lysine and Chondroitin Sulfate..... | 42 |
| 3.3.2. Layer-by-layer of Poly-L-Lysine and Heparin..... | 43 |
| 3.3.3. Layer-by-layer of Poly-L-Lysine and Hyaluronic Acid | 44 |
| 3.3.4. Grafting of Type I Collagen | 44 |
| 3.4. Morphological Characterization: Optical Microscopy | 46 |
| 3.5. Biochemical Characterization of Microspheres and their Functionalization | 47 |
| 3.5.1. Sample Preparation | 47 |
| 3.5.2. Thermogravimetric Analysis | 47 |
| 3.5.3. Data Analysis..... | 48 |
| 3.6. Cell Culture..... | 48 |
| 3.6.1. Culture Well Fabrication | 48 |
| 3.6.2. Cell Lines | 49 |

| | | |
|----------|---|----|
| 3.6.3. | <i>Thawing and Expansion of cells</i> | 49 |
| 3.6.3.1. | <i>Thawing and expansion of hMSCs</i> | 50 |
| 3.6.3.2. | <i>Thawing and Expansion of MMCs</i> | 51 |
| 3.6.4. | <i>Culture to Set the Operating Conditions</i> | 51 |
| 3.6.4.1. | <i>Experiment Setup</i> | 51 |
| 3.6.4.2. | <i>Trypan Blue Assay</i> | 52 |
| 3.6.5. | <i>Culture for the Validation of the Platform</i> | 53 |
| 3.6.5.1. | <i>Experiment Setup</i> | 53 |
| 3.6.5.2. | <i>MTS Assay</i> | 55 |
| 3.7. | <i>Drug Resistance Analysis</i> | 57 |
| 3.8. | <i>Statistical analysis</i> | 57 |
| 4. | <i>Results and Discussion</i> | 59 |
| 4.1. | <i>Morphological Characterization of Magnetic Microspheres: Size Distribution</i> | 59 |
| 4.2. | <i>Biochemical Characterization of Magnetic Microspheres: TGA</i> | 61 |
| 4.3. | <i>Cell Culture</i> | 65 |
| 4.3.1. | <i>Culture to Set the Operating Conditions</i> | 65 |
| 4.3.2. | <i>Cell Proliferation</i> | 67 |
| 4.4. | <i>Drug Resistance</i> | 69 |
| 5. | <i>Conclusions</i> | 73 |
| | <i>Bibliography</i> | 76 |

List of figures

| | |
|--|----|
| Figure 1. a) Bone marrow in the central cavity of a femur (created with BioRender.com). b) Representative example of bone marrow cellularity in the distal femur of normal adult B6C3F1 mice (adapted from [1]). c) Representation of the bone marrow vasculature (adapted from [1]). | 15 |
| Figure 2. Hematopoiesis. Pluripotent stem cells give rise to different types of mature blood cells through differentiation. Created with BioRender.com. Based on: [3]. | 16 |
| Figure 3. Maturation and differentiation process of B lymphocytes. Source: [5]. | 17 |
| Figure 4. Plasmatic cell and various non-Ig secreted factors that PCs produce and the biological processes that PCs are known to regulate. In red are represented the pro-inflammatory cytokines, in green the non-inflammatory ones. Source: [6]. | 18 |
| Figure 5. Organization of the bone marrow microenvironment and its components. Source: [10]. | 19 |
| Figure 6. Graphic representation of the evolution of multiple myeloma. Created with BioRender.com. Based on [29]. | 23 |
| Figure 7. Different microgel applications based on their organization: 3D encapsulation (A), cell expansion (B), transport of substances <i>in vivo</i> (C), assembled scaffolds (D), “lock and key” type shape (E), complementary molecular binding pairs (F). Source: [70]. | 31 |
| Figure 8. Alginate structure. Adapted from:[72]. | 31 |
| Figure 9. Assembly for the obtainment of microspheres with a close-up of the microfluidic system. Created with BioRender.com. | 40 |
| Figure 10. General scheme of the LbL process. Created with BioRender.com. | 41 |
| Figure 11. Functionalized microsphere through the layer-by-layer technique with a polycation (PLL) and a polyanion (CS/Hep/HA). Created with BioRender.com. | 44 |
| Figure 12. Functionalized microsphere through the layer-by-layer technique with the polycation PLL and the polyanion CS, and the final layer of Col I through the GA. Created with BioRender.com. | 46 |
| Figure 13. Hydrogels in p12 plates for cell culture. Created with BioRender.com. | 53 |
| Figure 14. Illustration of the cell culture in the hydrogels’ conic microwells showing the 5 different conditions: CTRL, MCR, DIR, COX, and COW. Created with BioRender.com. | 54 |
| Figure 15. Cell culture for the validation of the platform timeline. | 57 |
| Figure 16. A) Diameter distribution of non-functionalized alginate microspheres with ferrite. B) Microspheres observed under an inverted microscope on a scale of 100 μm . | 60 |
| Figure 17. Diameter distribution of alginate microspheres functionalized with CS (A), Hep (B), HA (C), and Col I (D) | 61 |

Glossary

| | |
|--------------------------|--|
| Abs | Antibodies |
| Alg | Alginate |
| ASC | Autologous stem cell transplant |
| ATCC | American type culture collection |
| BM | Bone marrow |
| BMECs | Bone marrow endothelial cells |
| BR | Biological replicate |
| CAFs | Cancer-associated fibroblasts |
| CAM-DR | Cell adhesion-mediated drug resistance |
| CBIT | Centre for biomaterials and tissue engineering |
| Col I | Type I collagen |
| COW | Indirect co-culture condition with microgel |
| COX | Indirect co-culture condition without microgel |
| CS | Chondroitin sulfate |
| CTRL | Control condition |
| DEX | Dexamethasone |
| D_f | Dilution factor |
| DIR | Direct co-culture condition |
| DMEM (medium) | Dulbecco's modified eagle collection |
| DMSO | Dimethylsulfoxide |
| DPBS | Dulbecco's phosphate-buffered saline solution |
| DR | Drug resistance |
| ECM | Extracellular matrix |
| EDC | N-(3-dimethylaminopropyl)-N'-ethylcarbodiimide |
| FBS | Fetal bovine serum |
| FV | Final volume |
| GAG | Glycosaminoglycan |
| GC | Glucocorticoid |
| Gly | Glycine |
| HA | Hyaluronicacid |
| Hep | Heparin |
| hMSCs | Human mesenchymal stem cells |

| | |
|---------------|--|
| HSCs | Hematopoietic stem cells |
| Ig | Immunoglobulin |
| iHDACs | Histone deacetylase inhibitors |
| IL | Interleukin |
| IMiDs | Immune-modulatory drugs |
| L-Glut | L-glutamine |
| LbL | layer-by-layer |
| mAbs | Monoclonal antibodies |
| MCR | Monoculture condition |
| MGUS | Monoclonal gammopathy of unknown significance |
| MM | Multiple myeloma |
| MMCs | Multiple myeloma cells |
| MO | Magnetic alginate microspheres |
| mPCs | Monoclonal plasma cells |
| MPP | Multipotent progenitors |
| MRD | Minimal residual disease |
| MSCs | Mesenchymal stem cells |
| MTS | it refer to both the cell viability assay and the compound 3-(4,5-Dimethylthiazol-2-yl)-5-(3-carboxymethoxyphenyl)-2-(4-sulfophenyl)-2H-tetrazolium that give the assay its name |
| NFκB | Nuclear factor kappa-light-chain-enhancer of activated B cells |
| NG | Neural-gial |
| NHS | N-hydroxysuccinimide |
| NK | Natural killer |
| NM | Normal medium |
| P/S | Penicillin/streptomycin |
| PCL | Plasma cell leukemia |
| PCs | Plasma cells |
| PEG | Polyethylene glycol |
| PIs | Proteasome inhibitors |
| PLL | Poly-L-lysine |
| Prx | Paired related homeobox |
| PVA | Polyvinyl alcohol |
| RCCSTM | Rotary cell culture system |

| | |
|----------------------|---|
| RPMI (medium) | Roswell park memorial institute |
| RRMM | Relapsed/refractory multiple myeloma |
| SDs | Standard deviations |
| SM | Super medium |
| SNS | Sympathetic nervous system |
| STAT | Signal transducer and activation of transcription 3 |
| TG | Thermogravimetric analysis |
| TGF | Transforming growth factor |

1. Introduction

1.1. Bone Marrow

The bone marrow (BM) is located in the central cavities of axial and long bones (Figure 1, a). It consists of hematopoietic tissue islands and adipose cells surrounded by vascular cavities that are traversed by a meshwork of trabecular bone (Figure 1, b), and it accounts for about 5% of body weight in humans. The BM is the most important hematopoietic organ and a primary lymphoid tissue [1].

Determining the spatial architecture of hematopoiesis in the BM is essential for comprehending how this tissue maintains gradual, balanced differentiation to satisfy organism demands.

The vasculature of bone marrow consists of unique arterioles that enter the bone and convert into transitional vessels, leading to an intricate network of fenestrated sinusoids that occupy a significant portion of the BM area. This vasculature is closely associated with a network of perivascular reticular cells that spread throughout the BM (Figure 1, c).

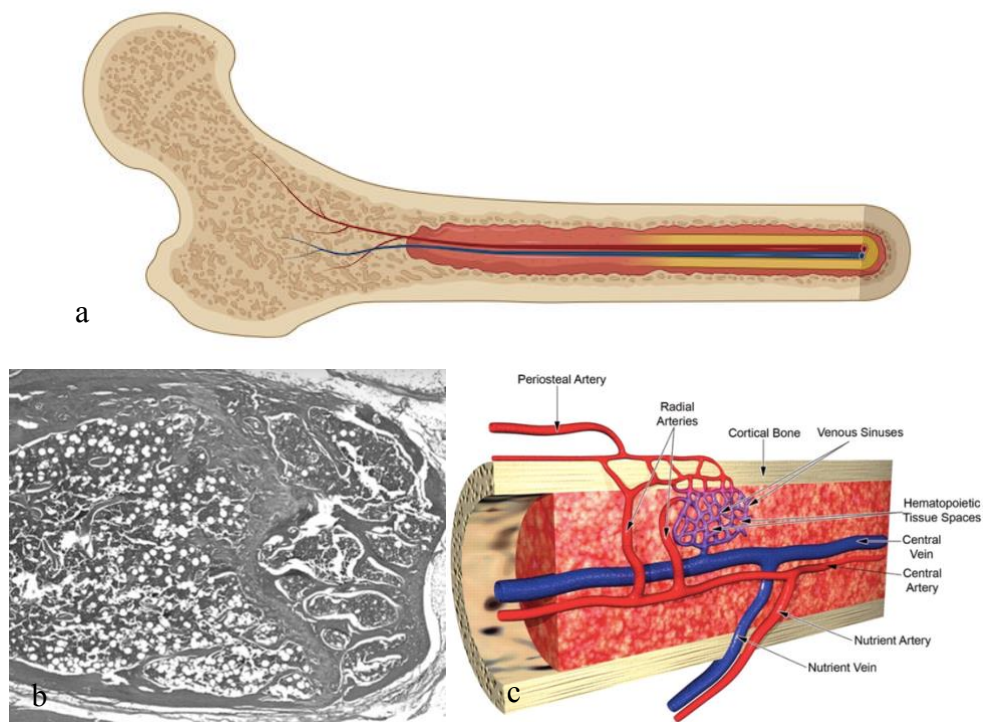


Figure 1. a) Bone marrow in the central cavity of a femur (created with BioRender.com). b) Representative example of bone marrow cellularity in the distal femur of normal adult B6C3F1 mice (adapted from [1]). c) Representation of the bone marrow vasculature (adapted from [1]).

The specialized vascular structure defines different areas, called niches, which provide a suitable environment for hematopoietic stem cells (HSCs), multipotent progenitors (MPP), and lineage-committed progenitors to self-renew and differentiate into various blood cells necessary to sustain life [2].

1.2. Hematopoiesis and Plasmatic Cells

The process of hematopoiesis occurs in the gaps between vessels, bone, and reticular cells in the BM [2]. The HSCs are at the top of a hierarchy of multipotent progenitors that become progressively more restricted to several committed precursors or single lineages that give rise to the different types of mature blood cells (Figure 2) [3].

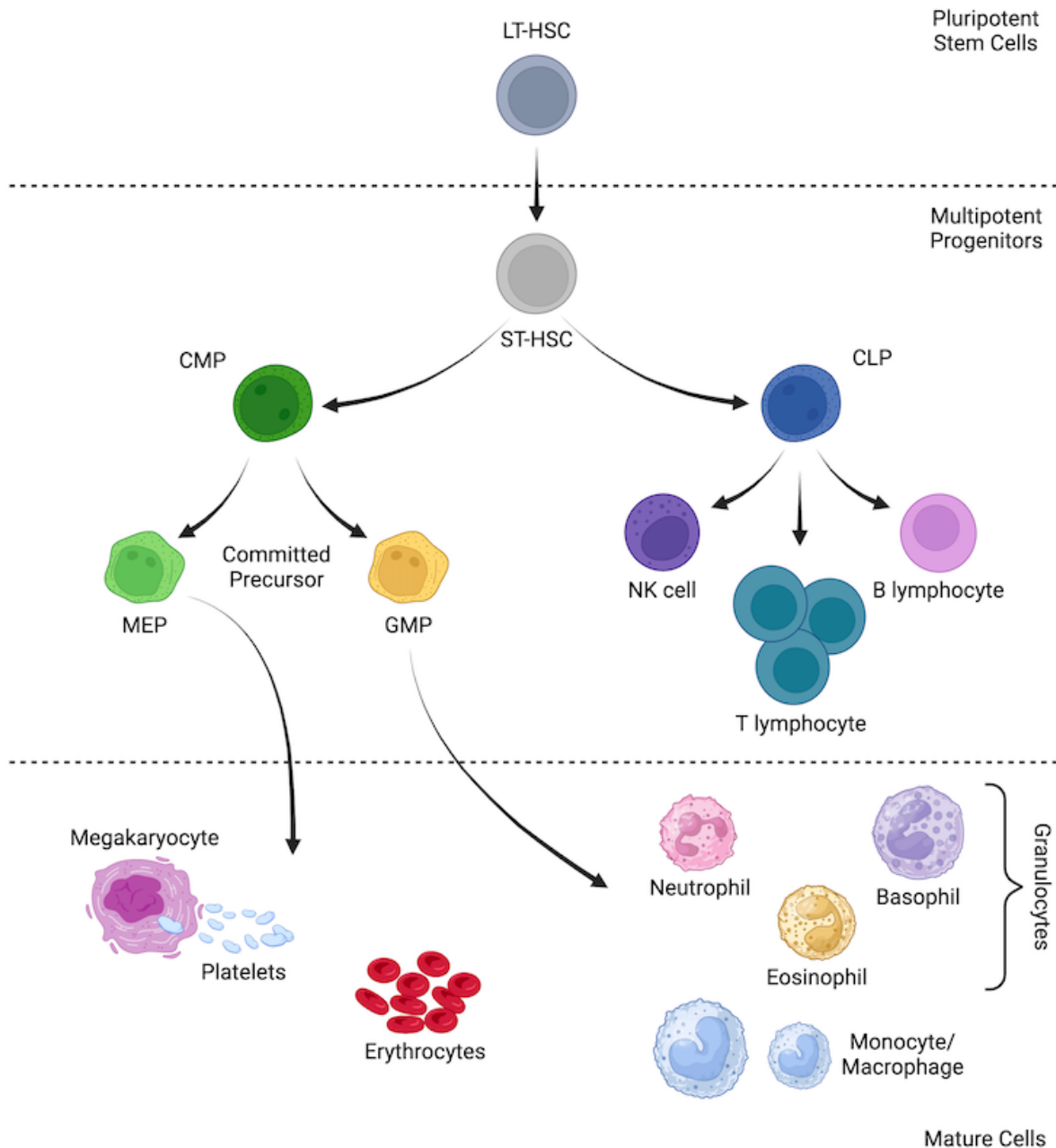


Figure 2. Hematopoiesis. Pluripotent stem cells give rise to different types of mature blood cells through differentiation. Created with BioRender.com. Based on: [3].

Plasma cells (PCs) are the final stage of development for mature B lymphocytes. They produce a significant amount of antigen-specific antibodies (Abs), which are essential for both short and long-term humoral immunity [4].

The primary role of B lymphocytes is to produce immunoglobulins (Igs), which are essential for protecting the body against a range of pathogenic microbes. Their absence can be fatal if not compensated for by repeated lifelong injections of human immunoglobulins. This condition can be caused by abnormal B cell differentiation, known as variable common immunodeficiency, or a lack of B cells, called severe combined immunodeficiency or X-linked agammaglobulinemia.

The natural development of B lymphocytes can be divided into two main stages (Figure 3). The fetal liver and adult bone marrow are the sites of the first step, known as B lymphopoiesis. It allows hematopoietic multipotent stem cells to commit and grow into mature B lymphocytes co-expressing IgM and IgD. It remains largely unaffected by antigens and T lymphocytes.

The second stage is called immunopoiesis and it takes place mainly in secondary lymphoid organs such as lymph nodes, spleen, Peyer's patches, and tonsils. Resting B cells are stimulated by antigen invasion, which leads to their expansion and the expression of new cell surface markers. Upon entering the cell cycle (blast stage), they begin to divide rapidly in response to the additional stimulation, compensating for the comparatively small amount of antigen-specific B cells that are normally available. Ultimately, these cells develop into antibody-secreting plasmablasts. The bone marrow and mucosa are the targets of the plasmablasts produced in these organs, where they develop into non-dividing plasma cells (PCs) [5].

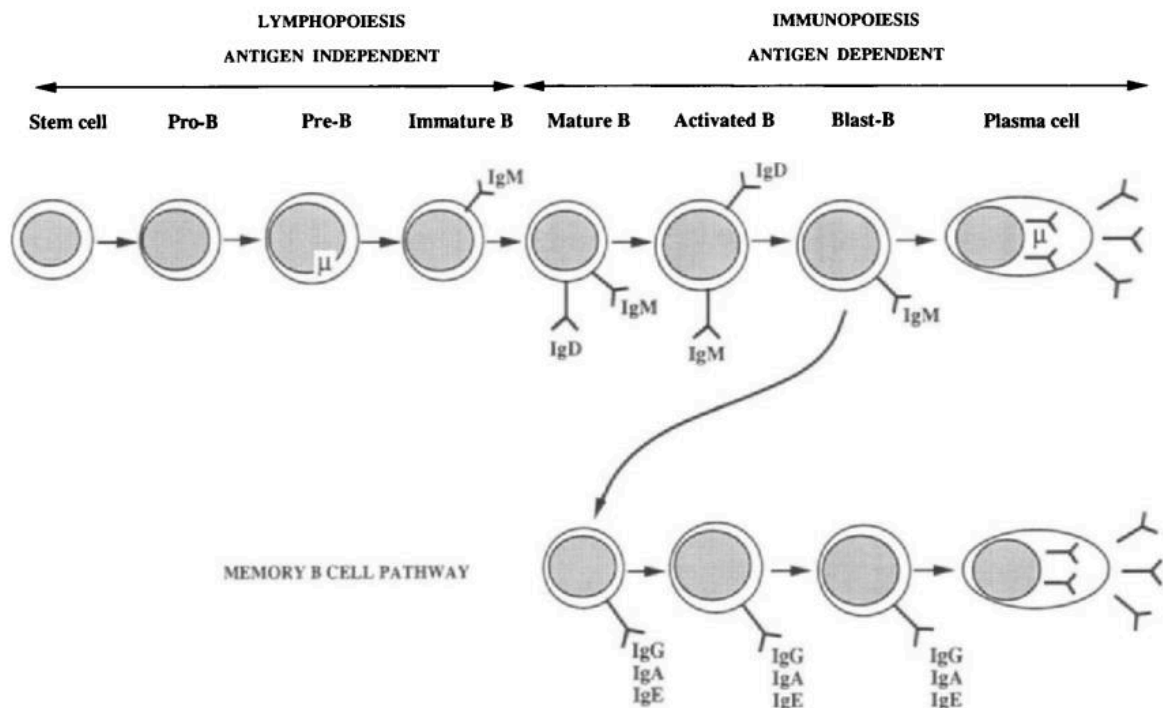


Figure 3. Maturation and differentiation process of B lymphocytes. Source: [5].

The ability to secrete large amounts of Abs and have a long-life span makes PCs most recognizable and makes them an essential component of humoral immunity. [6].

During their two to three days lifespan, they continuously synthesize and secrete antibodies that are specific for the antigen that stimulated the plasma cell precursor to proliferate and differentiate. It is believed that a single plasma cell is capable of secreting hundreds to thousands of antibody molecules per second, which is astonishing evidence of the effectiveness of the immune response in defending against infection [7].

However, it is now known that PCs fulfill other functions in addition to antibody secretion. They can have profound effects on both pathological and non-pathological processes. According to recent studies, PCs play a crucial role in the regulation of processes such as neuroinflammation and hematopoiesis. PCs have been found to express cytokines, including IL-17, IL-35, and IL-10. Apart from ILs and IGs, PCs can also produce and secrete other factors [6] as illustrated in Figure 4.

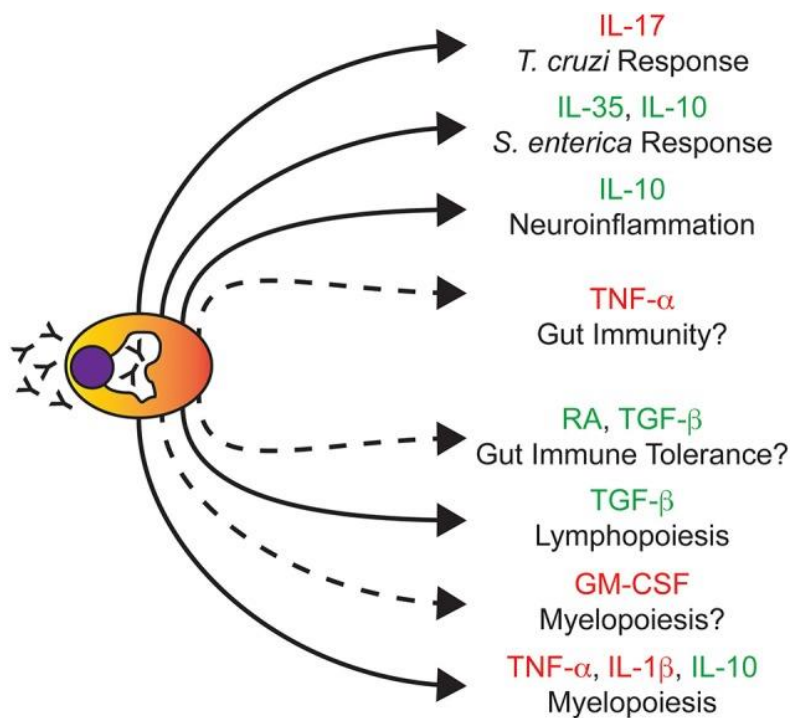


Figure 4. Plasmatic cell and various non-Ig secreted factors that PCs produce and the biological processes that PCs are known to regulate. In red are represented the pro-inflammatory cytokines, in green the non-inflammatory ones. Source: [6].

1.3. Bone Marrow Composition

The BM microenvironment represents a very complex organization (as shown in Figure 5) that serves as a vital and dynamic system that supports hematopoiesis. Both cellular and non-cellular components regulate and influence different functions characterizing HSCs, in particular localization, proliferation, quiescence, differentiation, and self-renewal [8], [9].

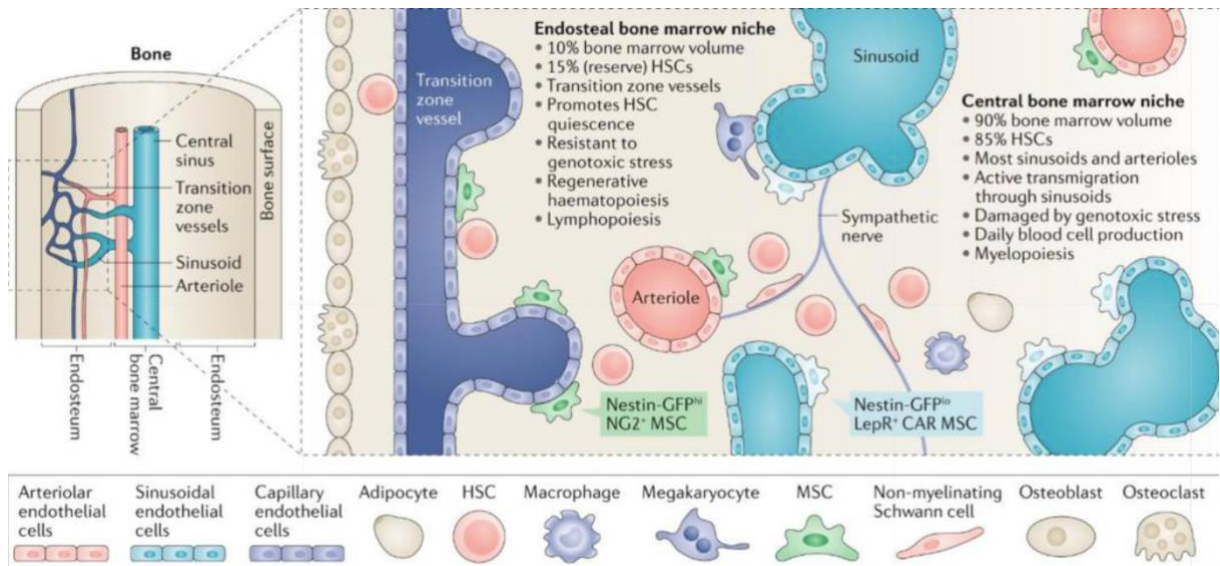


Figure 5. Organization of the bone marrow microenvironment and its components. Source: [10].

1.3.1. Cellular Component of Bone Marrow

The BM is composed of various types of cells, including hematopoietic and mesenchymal stem cells. These cells interact with each other to regulate the formation of blood and bones. Hematopoietic stem cells require specific cellular microenvironments, including osteoblasts, adipocytes, endothelial cells, and nerves, to carry out their functions. Additionally, bone remodeling is organized by a collective effort of osteoblasts, osteoclasts, osteocytes, and endothelial cells [11].

Osteoblasts are cells of mesenchymal origin and play a crucial role in the endosteal niche as they are the primary contributors and act as the first point of contact between the calcified bone and the BM. They are responsible for new bone formation and have been identified as key players in the regulation of hematopoiesis for a long time. Recent studies suggest that osteoblasts may regulate hematopoiesis differently depending on their differentiation state [3], [11].

Osteoclasts are terminally differentiated multinucleated cells, which originate from mononuclear cells of the hematopoietic stem cell lineage as a result of multiple steps. Their main function is bone-resorbing, but recent studies demonstrate that they may also directly regulate the hematopoietic stem cell niche [12].

BM adipocytes make up about 70% of marrow space in adults and serve as a key component of the bone marrow microenvironment for hematopoietic stem cells [11]. Nowadays, it is widely accepted that the number of adipocytes in BM increases with age and due to various signals. In some cases, these changes have been linked to a decrease in bone mass. Moreover, BM adipocytes have been identified as negative regulators of hematopoiesis.

This suggests that they play an important role not only in the BM environment but also in maintaining overall body homeostasis [13].

Endothelial cells play a crucial role in regulating organ homeostasis, promoting regeneration through direct interaction with local stem and progenitor cells, and secretion of angiocrine factors. BM endothelial cells (BMECs), create a physical barrier that prevents mature red blood cells and platelets from entering the bone marrow from circulation. This barrier regulates the movement of cells and is crucial for processes such as hematopoiesis and osteogenesis. BMECs also play a role in the specialized perivascular microenvironments where the majority of hematopoietic stem and progenitor cells in the bone marrow reside [14].

The sympathetic nervous system (SNS) innervates the BM and plays a crucial role in the circadian mobilization of HSCs [15]. Bone marrow sympathetic nerves release noradrenaline, promoting HSCs release from the niche. The non-myelinating Schwann cells surrounding the periarteriolar sympathetic nerve fibers activate a dormant form of the transforming growth factor- β (TGF- β) protein that helps in maintaining the quiescence of HSCs [16].

1.3.1.1. Mesenchymal Stem Cells

Stem cells are characterized by their ability to differentiate into various lineages and to self-renew [17]. Mesenchymal stem cells (MSCs) are a dynamic population of cells capable of self-renewal, differentiation, tumor and wound homing, and immunomodulation [18].

These cells have multipotent capabilities and play a significant role in tissue repair [15]. They can be found in many organs of the body, including the BM. Harvested from bone BM, adipose tissue, cord blood, or a variety of other sites, MSCs play multiple roles in tumor progression, and they can have both tumor-supportive (pro-tumor) and inhibitory (anti-tumor) effects [18]. MSCs possess the ability to differentiate into a variety of non-hematopoietic cell types, such as osteoblasts, chondrocytes, and adipocytes, and *in vitro*, they give rise to the bone marrow stromal cells as well [19]. MSCs can be identified by specific markers such as Nestin, Neural-Glial Antigen (NG)-2, Leptin Receptor, or Paired Related Homeobox (Prx-1). They are typically found in the bone marrow close to the vasculature. MSCs secrete various growth factors, cytokines, and chemokines that play a crucial role in immunomodulation, cell migration, proliferation, and differentiation [15], [20].

Beyond their important pluripotent potential, most myeloma-specific studies demonstrate a stimulatory, protective, and pro-tumor effect of MSCs on myeloma cells, suggesting that novel drugs could counteract these tumor-supporting effects in the bone marrow. In fact, bone marrow-derived MSCs interact directly with MM cells resulting in secretion of cytokines,

chemokines and adhesion molecules that support growth and proliferation of the tumor cells [18], [19].

1.3.2. Bone Marrow Extracellular Matrix

The extracellular matrix (ECM) of the BM is created by niche cells and interacts with a range of molecules, including secreted proteins and membrane-bound proteins with large extracellular domains. The BM contains several abundant ECM proteins such as fibronectin, collagens (I-XI), laminin, tenascin, thrombospondin, and elastin. Proteoglycans with their large glycosaminoglycan (GAG) side chains, like hyaluronic acid, chondroitin sulfate, dermatan sulfate, heparan sulfate, keratan sulfate, and heparin, are also critical for the integrity of the ECM. Other molecules associated with the ECM are the soluble or membrane-bound glycoproteins of the sialomucin family; these include CD34, GlyCAM1, MadCAM1, PSGL1/CD162, SPN/CD43, CD45RA, and CD164. Integrins and selectins are essential for cell-cell and cell-matrix interactions in the BM. In contrast, membrane-bound receptors of the immunoglobulin superfamily, such as ICAM1 (CD54), VCAM1 (CD105), and CD166, also contribute to shaping the bone marrow niche [21].

Various studies have demonstrated that the extracellular matrix (ECM) plays a crucial role in regulating the behavior of hematopoietic stem cells. The ECM influences HSCs activity both directly, by interacting with ligands to provide instructive signals, and indirectly, by sequestering growth factors and cytokines that would otherwise activate the cells. This relationship between HSCs and ECM is a two-way system, meaning that the ECM not only affects HSCs, but the stem cells themselves are also capable of modifying the niche in response to their signals [22].

1.4. Multiple myeloma

Multiple myeloma (MM) is a clonal plasma cell malignancy that accounts for slightly more than 10% of all hematologic cancers [23]. It is characterized by the uncontrolled proliferation of monoclonal plasma cells (mPCs) in the BM, affected in their transformed state, which leads to an excess of immunoglobulin (Ig) chains or non-functional intact immunoglobulins detectable in biological fluids like blood and/or urine [19], [24].

The undisciplined growth of mPCs is largely attributed to the BM niche and is associated with serum monoclonal gammopathy (M-spike) and organ dysfunctions. This can cause destructive bone lesions, kidney injury, anemia and hypercalcemia [25], [26].

The multistage evolution of MM pathophysiology includes several stages (Figure 6). It starts with monoclonal gammopathy of unknown significance (MGUS), followed by asymptomatic (smoldering) MM, symptomatic (intramedullary) MM, and extramedullary MM/plasma cell leukemia (PCL). Smoldering MM is an intermediate stage between MGUS and active MM, and although it doesn't show symptoms of MM, it can often progress into overt symptomatic MM after varying periods of time. Symptoms of MM include anemia, lytic bone lesions (mainly in the axial skeleton) and diffuse osteoporosis, hypercalcemia, renal dysfunction (due to monoclonal Ig deposition), and an increased risk of infection. Advanced disease can cause malignant PCs to develop extramedullary lesions (e.g. plasmacytomas in soft tissue) and can also be found as PCL in the bloodstream [24].

Intraclonal heterogeneity is a common feature of MM, that adds an extra layer of complexity to the disease progression. This heterogeneity suggests the possibility that mPCs randomly generate genetic mutations to create populations of subclones, resulting in the selection of those with aberrations that offer a higher chance of surviving cells [27]. The reason can be connected to the emergence of clinical relapses because if treatments are selected to target a particular mutation in the tumor cells, the primary clone would be impacted while residual clones that might otherwise lead to the disease's reappearance would remain unaffected [28]. The interaction between tumor cells and the microenvironment has been shown to initiate these secondary genetic events that promote the disease's progression in its early stages [27]. Therefore, the development of the disease is influenced by both spontaneous intracellular genetic alteration and the interaction of mPCs with the microenvironment.

1.1. Multiple Myeloma Treatments

Despite the dramatic improvement in patient outcomes with myeloma-targeted and immunomodulatory agents, MM remains largely incurable [30]. After induction therapy, autologous stem cell transplant (ASCT) remains the standard of care for eligible MM patients. There has been a significant increase in the number and variety of treatments available for MM in recent years. This has changed the treatment landscape considerably. Although MM is still incurable, the expansion of effective treatments means it can often be controlled over the long term [31].

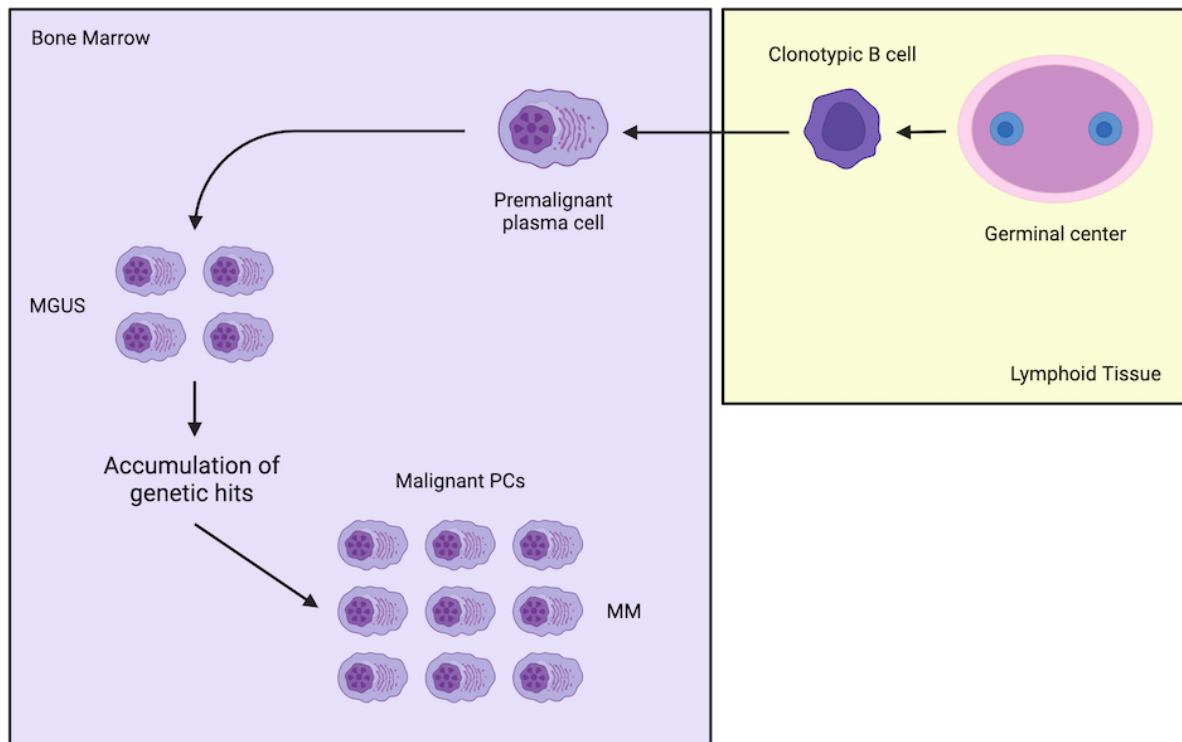


Figure 6. Graphic representation of the evolution of multiple myeloma. Created with BioRender.com. Based on [29].

The treatment of MM typically involves a combination of drugs that have different mechanisms of action. These drugs include corticosteroids, alkylating agents, anthracyclines, proteasome inhibitors (PIs), immuno-modulatory drugs (IMiDs), histone deacetylase inhibitors (iHDACs), monoclonal antibodies (mAbs), nuclear export inhibitors and high-dose chemotherapy that are rescued by autologous stem cell transplantation. The use and optimization of combinations of these drugs have led to an improvement in the overall survival of patients with MM. The median survival rate was 2.5 years before 1997, 4 years in the following decade, and more recently over 7 years. Currently, patients newly diagnosed with multiple myeloma are usually treated with induction therapy, which typically consists of three different drugs, such as bortezomib, lenalidomide and dexamethasone [32].

Unfortunately, most patients who experience a prolonged response after initial therapy will eventually relapse or become resistant to treatment [31].

Relapsed/progressive MM acquires additional mutation or genetic alterations that render the disease more resistant, leading to progressively shorter durations of remission or response to each salvage therapy, and the ultimate development of relapsed/refractory MM (RRMM). For this reason, new combinations of next-generation novel agents and/or antibodies are undergoing clinical trials [33].

1.1.1. Dexamethasone

Dexamethasone (DEX) is a glucocorticoid (GC) widely used in MM treatment. DEX is commonly used in combination with thalidomide to treat newly diagnosed MM patients as the combination regimen shows significantly superior response rates compared to DEX alone. As a GC, the effect of DEX occurs through its binding to the GC receptor and its action induces apoptosis in MM cells. After GC binds the receptor, it translocates to the nucleus and interacts with GC-response elements to induce gene transcription (transactivation). Alternatively, GC receptor directly interacts with transcription factors, like nuclear factor kappa-light-chain-enhancer of activated B cells (NFkB), to suppress their activity (transrepression). The transactivation activity of GC receptor is highly regulated and is essential for GC-induced apoptosis involving the intrinsic mitochondrial pathway [34].

1.2. Tumor Microenvironment

The tumor microenvironment plays a crucial role in the development and progression of MM. Myeloma cells grow and expand almost exclusively in the bone marrow, which underscores the importance of the bone marrow microenvironment in supporting myeloma cell growth and survival. In this microenvironment, there is a complex interaction involving bidirectional positive and negative communication among the many cell types present. The microenvironment can be functionally divided into a cellular and non-cellular compartment, each of which has components that play distinct but interacting roles in the progression of MM. The cellular compartment is composed of two cell types, the hematopoietic and non-hematopoietic cells. The first of these include myeloid cells, T and B lymphocytes, natural killer (NK) cells, and osteoclasts, while the non-hematopoietic cell types include bone marrow stromal cells, marrow-derived mesenchymal stromal cells, fibroblasts, osteoblasts, adipocytes, endothelial cells, and the blood vessels. The non-cellular compartment includes the extracellular matrix and the various cytokines, chemokines, growth factors, and exosomes that are produced by the cellular compartment [19].

1.3. Drug Resistance in Multiple Myeloma

Initially, most patients with MM respond to anti-myeloma treatment, but they eventually develop resistance to subsequent treatments [35]. There are several reasons why multiple myeloma can become resistant to drugs. The main causes of drug resistance (DR) are:

- I. Genetic and epigenetic alterations.

- II. Abnormal drug transport and metabolism, that lead to a decrease in the amount of drugs that reach the inside of the cells.
- III. Dysregulated apoptosis or other intracellular signaling pathways, and activation of autophagy.
- IV. Persistence of cancer stem cells to most drugs, which can cause self-initiating MM.
- V. Dysfunctional tumor microenvironment, dependent on MM cells and stromal microenvironment components.
- VI. Specific mechanisms for immunotherapies with antibodies.

DR is the main cause of relapses in MM patients [32].

It is crucial to comprehend the mechanisms that underlie DR in MM and establish more effective therapeutic approaches [35].

This thesis will focus on the interactions between MM cells and other cells in the tumor microenvironment for realistic testing of antitumoral drugs and better comprehending the tumor microenvironment's role in DR.

1.3.1. Influence of the BM Microenvironment on Drug Resistance

The BM microenvironment encourages mechanisms that increase PCs lifespan through cell-cell and cell-environment interactions. On the other hand, in MM patients, the disease's growth and progression are encouraged by the interaction between the mPCs and the BM microenvironment. The primary survival and proliferation factor for mPCs, both *in vivo* and *in vitro*, is interleukin-6 (IL-6), which is mainly produced by the stromal environment and the MM cells themselves. However, the IL-6 is not sufficient to ensure mPCs survival. The reason why the disease progresses can be attributed to the presence of a tumoral microenvironment where the cells that form the microenvironment, in addition to mPCs, are also abnormal. The result is a vicious circle, whereby each cell type contributes to the growth of the tumor [36], [37].

The MM environment consists of various interactions that support not only the disease maintenance and growth but also the development of DR, obstructing the effective treatment of MM and encouraging relapse [36]. The cause of the relapses is to be attributed to the clinical condition called minimal residual disease (MRD), which refers to the persistence of disease undetectable by standard morphology-based diagnostic tests, requiring additional sensitive techniques [38]. The DR can be acquired or *de novo*. Acquired drug resistance is often manifested by multifactorial resistant mechanisms, making it therapeutically difficult to reverse. It occurs as a result of sequential genetic and epigenetic changes that predispose tumor cells to survive initial drug exposure and acquire a more complex and permanent DR phenotype

[36], [39]. De novo DR exists prior to any treatment exposure and selection for DR. It is produced due to the interaction of mPCs with the cellular microenvironment. This microenvironment protects the cells from chemotherapy, radiotherapy or receptor-targeting drugs due to the presence of soluble factors that mediate DR or by the adhesion of mPCs to stromal cells and/or to the ECM components, a process known as cell adhesion-mediated drug resistance (CAM-DR) [36], [39], [40].

1.3.2. Interactions Between mPCs and ECM Components and their Effect on CAM-DR

It has been reported that several biomolecules that are part of the ECM participate in CAM-DR. Since ECM molecules are naturally occurring polymers that can be included into 3D tissue engineering techniques for *in vitro* disease modeling, their study is extremely pertinent to this thesis.

Considering the mPCs-ECM interactions and the CAM-DR effect, we can include different molecules such as hyaluronic acid (HA), chondroitin sulfate (CS), type I collagen (Col I) and heparin (Hep).

HA, a non-protein GAG formed from repeating disaccharide units of N-acetyl-D-glucosamine and D-glucuronate [41], is a major component of the ECM in mammalian BM. GAGs can bind to growth factors and cytokines that are involved in the generation of DR and then increase their activities. The primary effect of HA is mediated by IL-6 because of its high water-absorbing capacity. HA concentrates and retains this cytokine near to its site of secretion, which promotes its autocrine activity. On the other hand, HA also takes part in CAM-DR via direct interaction with mPCs, mediated by the adhesion molecule CD44 [42]. HA-mediated survival and proliferation of mPCs is related to a down-regulation in the expression of p27kip1 and a hyperphosphorylation of the retinoblastoma protein [43].

Adhesion of mPCs to HA has also been linked to activation of Wnt/ β -catenin and resistance to lenalidomide, as well as DR against DEX mediated by various signaling pathways, causing signal transducer and activator of transcription 3 (STAT3) phosphorylation in MM cell lines that are IL6-dependent, while resistance in MM cell lines that are IL6-independent is caused by upregulation of Bcl-2 and activation of the NF κ B pathway [44].

CS is a sulfated GAG that is widely distributed on cell surfaces and in the ECM in the form of proteoglycans, which is composed of a panel of core proteins, and at least one CS side chain

that is covalently attached to them [45]. CS is a linear polysaccharide consisting of repeating disaccharide units of glucuronic acid and N-acetyl galactosamine residues linked by β bonds. There are various forms of CS depending on which residue of N-acetyl galactosamine is sulfated. Chondroitin-6-sulfate, or chondroitin sulfate C, is the more prevalent type in the BM niche [46]. Due to their negatively charged hydrophilic nature, CS chains have long been thought to contribute to hydrate matrix formation. This can be achieved through organizing local microenvironments for almost all cell types or by preventing compressive loads. However, the unique sulfation pattern of the CS chains defines the spatial arrangement of the negative charges on the GAG polymer backbone, providing them with additional functional properties to physically interact with many extracellular and pericellular molecules [47]. In addition to providing structural function, CS also acts as an intermediary in the regulation of various cellular processes, exhibiting immunomodulatory and anti-inflammatory properties. Although testing in traditional 2D cultures has not revealed the impact of CS on MM cell lines' resistance to drugs [42], it would be interesting to investigate this biomolecule's function in more biomimetic *in vitro* settings.

Collagen is a fibrous protein and an essential structural component of all connective tissue. 28 different types of collagens have been identified, creating a unique ECM composition in different tissues. Col I, the most abundant in the human body and the most prevalent component of the ECM, is a heterodimer assembled from two identical $\alpha 1$ chains and one $\alpha 2$ chain [48], [49]. Collagen involvement in cancer progression has been widely documented, mostly about solid tumors. New research suggests that fibroblast-derived collagens and so-called cancer-associated fibroblasts (CAFs) play a major role in the development of tumors and response to treatments [49]. Because of its ability to interact with various cellular types in the BM ECM, including HSCs and MSCs, Col I has been included in a variety of *in vitro* models of the bone marrow niche (BMN) [50]. Regarding MM, plasmatic cells interact with Col I by syndecan-1 [51], which is a critical player in the interaction between MM cells and their BM niche. Syndecan-1 recently has been shown to promote Wnt/ β -catenin signaling, which is associated with MM proliferation, dissemination, DR, and disease progression [52]. According to a study conducted by Marín-Payá J. C. et al. [53], collagen has been found to induce DR, even though it has no discernible effect on proliferation. The study highlights the significance of collagen in resistance development to DEX and concludes that collagen plays a significant role in this process, which could have important implications for MM treatment.

Heparin is a sulfated polysaccharide belonging to the glycosaminoglycans family and interacts with plasma proteins and tissue components to perform its several biological functions. It is composed of a mixture of chains of different lengths consisting of alternating residues of an uronic acid (L-iduronic acid; D-glucuronic acid) and a hexosamine (D-glucosamine). As a result, its structure cannot be simply described in terms of a unique sequence of carbohydrate residues [54]. There has been some progress in treating various cancers with heparin and heparin-like molecules. Understanding how these compounds might be used in future treatments is made easier by the pathways and mechanisms by which they prevent the growth of cancer cells [55]. Due to its unique structural features, Hep can bind a variety of bioactive molecules including growth factors and chemokines, which control important cell behaviors in both normal and pathological processes. This capacity to modulate numerous growth factor signaling pathways makes Hep play a significant role in the regulation of the tumor microenvironment by controlling tumor growth, angiogenesis, and metastasis [56], [57].

1.4.2D and 3D Culture Systems

As a crucial aspect of the drug discovery process, cell-based assays offer a quick, easy, and affordable alternative to expensive, time-consuming animal testing. Since the results of this technique rely on cellular responses to drugs, compounds, and external stimuli, the key element is cultured cells. Traditional 2D cell culture provides advantages such as cost-effectiveness, high-throughput screening, and standardization. However, even though 2D cell culture has been a widely used method in cell-based research, its limitations are becoming progressively recognized [58], [59].

More than 20 years of research have demonstrated that the distance between physiological tissues and cell cultures is shortened when cells are grown in 3D scaffolds. This is crucial, as drug responses assessed in 2D cultures may be overestimated [60], [61].

The *in vivo* architecture and microenvironment's lack of reproducibility is one of the main reasons 2D cultures are not representative [62] since they typically involve the growth of cells in a monolayer on glass or, more frequently, in tissue culture polystyrene plastic flasks [58]. For instance, 2D cultured tumor cells frequently exhibit reduced drug resistance and slower tumor progression when compared to tumors *in vivo*, which results in a discounted effectiveness of drug screening and testing [63]. Therefore, results from 2D cell culture experiments can occasionally be unpredictable and misleading when it comes to *in vivo* responses [58].

For these reasons, it is critical to create 3D *in vitro* culture systems that can reproduce *in vivo* cell behaviors more closely and yield more consistent results for *in vivo* tests [60].

One example of the 3D models is represented by organotypic cultures which have the advantage to preserve several aspects of the original tissue's structural and synaptic organization [64]. Among the most common and versatile methods in 3D culture can be also found spherical cell clusters formed by self-assembly, known as spheroids [65]. Cell spheroid is the key feature that replicates *in vivo* cells for further simulating cell differentiation, proliferation, and function *in vitro*. Spheroids typically exhibit internal gradients of proliferation, oxygen, nutrition distribution and metabolic waste accumulation. While the distant inner cells remain quiescent or die through necrosis and apoptosis, the peripheral cells closely mimic the *in vivo* microenvironment of actively proliferating tumor cells adjacent to capillaries. Because of this, 3D spheroid culture is an improved model for predictive *in vitro* cell-based assays and has the potential to provide preclinical drug discovery with high physiological relevance, particularly in the field of cancer research [62], [65]. However, for larger periods of cell culture with spheroids, the viability can be reduced due to the lack of oxygen and nutrients as well as the accumulation of residues in the core of the spheroid as it grows [58], [66].

Another important factor to consider, in addition to the cell-cell contact, is the interaction between cells and components of the ECM, which must be introduced in the *in vitro* models. Currently, many approaches to tissue engineering rely on the use of hydrogels and material scaffolds. These 3D structures function as a synthetic ECM, directing the growth and formation of a desired tissue by presenting stimuli and arranging cells into a 3D architecture. Numerous synthetic polymers, including polyethylene oxide, polyvinyl alcohol (PVA), and polyacrylic acid, as well as naturally derived materials, including HA, collagen, gelatin, alginate, and agarose, have also been used to create microporous scaffolds [67].

The use of microcarriers is one of the culture techniques implied to promote cell-ECM adhesion. They consist of microspheres composed of various crosslinked substances, typically with a diameter of 90-350 μm , which have a surface chemistry that encourages the growth of anchorage-dependent cells [68]. The application of various techniques and materials for surface modification of microcarriers has been the main focus of research efforts to improve cell attachment to microcarriers. the microspheres can be suspended in a culture medium and gently stirred to functionalize them using materials based on ECM. The adhesion of the cell to the microcarrier brings the cells to proliferate in a monolayer culture, even though they are cultured in suspension. Furthermore, due to their high surface-to-volume ratio, high cell densities are achieved in relatively low volumes. Additionally to the chemical properties, it has also been shown that cell adhesion and behavior depend on surface physical characteristics including curvature, topography, and rugosity as well as stiffness and elastic modulus [69].

Micron-sized hydrogels are becoming multifunctional platforms that can replicate tissue heterogeneity in artificial cell microenvironments [70].

Despite this, studies conducted in 2D cultures demonstrate the significance of the material's stiffness, as this parameter will encourage MSCs differentiation into distinct lineages: rigid surfaces (stiffness of 34 kPa) encouraged in a spindle-like shape of MSCs and osteogenic differentiation, low stiffness of 1 kPa promoted chondrogenic, adipogenic, and neuronal differentiation, and intermediate stiffness resulted in muscular lineage [69].

1.4.1. Microgel

Microgel refers to the aggregation in an aqueous medium of micrometer-sized particles. They are cross-linked polymeric spheres, biocompatible and with interesting properties, that can contain liquids and other substances inside. Individual microgels can serve as independent cell culture units in which cells are seeded onto the microgel's surface or encapsulated within it. It is possible to modify specific microgel properties to accommodate various cell types, enabling co-culture models within a single microgel. One of the most interesting properties of microgel is the ability to simulate the ECM of liquid-viscous tissues since they can also be fabricated from its components. Other features such as mechanical properties similar to soft tissues and the ability to incorporate cellular adhesive sites and to exchange substances with the environment are also noteworthy [70], [71].

One of the strengths of microgels is that they provide a multitude of design parameters that can be adjusted to suit different applications in tissue engineering (Figure 7) [70].

There are numerous established and well-recognized techniques for creating microgel systems, including emulsion, coacervation, gelation, spray drying, grinding, and microfluidics.

Microgel particles have recently been produced at sizes ranging from the nanoscale to the more widely used microscale. It has been demonstrated that the morphology of microgel particles is a readily manipulable variable that is essential to defining the porosity of microgel systems. Microgels can crosslink chemically or physically, and this contributes to the system's structure. A wide range of materials, including synthetic polymers like polyethylene glycol (PEG) and naturally occurring polysaccharides like chitosan and alginate, have been used to create microgels [71].

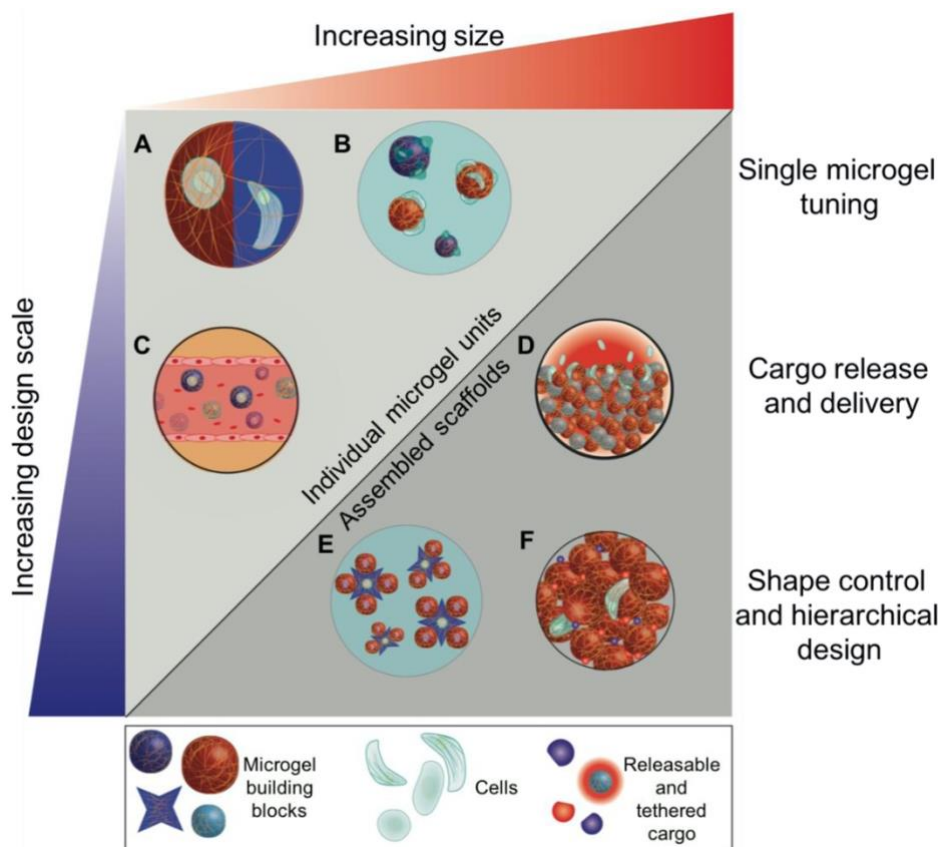


Figure 7. Different microgel applications based on their organization: 3D encapsulation (A), cell expansion (B), transport of substances in vivo (C), assembled scaffolds (D), “lock and key” type shape (E), complementary molecular binding pairs (F). Source: [70].

Alginate is a polysaccharide that consists of linear residues of β -D-mannuronic acid (M) and its C5-epimer α -L-guluronic acid (G) linked by 1 \rightarrow 4 glycosidic bonds, as shown in Figure 8. They are not repetitive units, and their order can vary: the molecular structure can contain blocks of consecutive G or M monomers (-GGG- or -MMM-) or blocks of alternating monomers (-MGMG-) [72].

Since it’s a polysaccharide, its charge is negative at neutral pH, which is an intriguing aspect of a functionalization process.

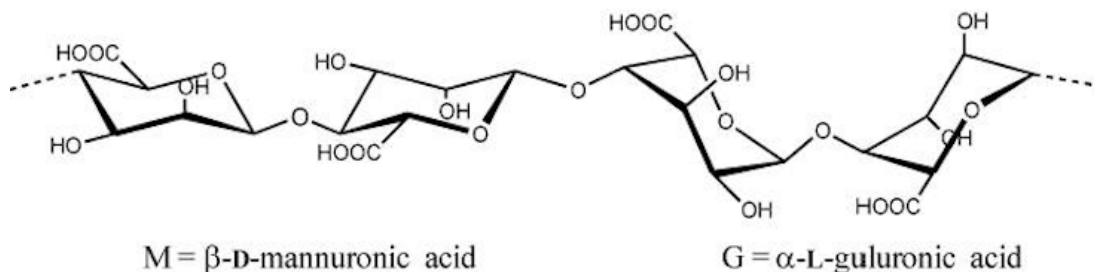


Figure 8. Alginate structure. Adapted from: [72].

Alginate exhibits exceptional qualities such as gel formation ability, non-toxicity, biodegradability, and ease of processing. Owing to alginate's superior qualities, sodium alginate, alginate hydrogels, and other materials based on alginate are used in a variety of biomedical domains, particularly in tissue engineering and drug delivery. Alginate can be easily

processed to create hydrogels, microspheres, microcapsules, sponges, foams, and fibers and, by using certain physical and chemical techniques, it can be blended and modified. The resulting new materials with alginate derivatives have distinct structures, functions, and enhanced mechanical strength, cell affinity, and gelation property [73].

1.5.3D Multiple Myeloma Culture Platforms

Multiple myeloma primarily develops inside the bone marrow microenvironment, which provides pro-survival signals and leads to drug resistance. 3D cultures that mimic multiple myeloma-bone marrow interactions are required to understand MM pathogenesis and drug response [61]. As a result, tissue engineering techniques have worked for decades to replicate the clinical issue of DR generation *in vitro*, attempting to include MM interactions with BM resident cells and BM ECM in the reconstruction of the MM microenvironment. These methods have mainly used hydrogel-based cultures, microfluidics devices, scaffolds, or 3D cultures of isolated MM cells in scaffolds in the microgravity-based rotary cell culture bioreactor system, as well as 3D cultures of human MM tissue explants [74].

In a study conducted by Jakubikova et al. in 2016 [75], a 3D culture model was developed co-culturing MM patient BM cells with MSC in a hydrogel 3D system composed mainly of laminin and collagen IV plus growth factors. Following the MSC expansion process, the mononuclear cell fraction is extracted from a BM aspirate obtained from patients with MM, where the monoclonal PCs are located. This fraction is then added to the hydrogel's surface to create a static three-dimensional system consisting of mesenchymal and mononuclear cells (cellular components), and noncellular components for the ECM components of the hydrogel.

Kirshner et al. in 2008 carried out a static 3D culture, coating the bottom of the wells with ECM components like fibronectin and type I collagen. This allowed them to later add the portion of MM patients' mononuclear cells that were encapsulated in fibronectin-based matrix [76].

As demonstrated by de la Puente et al. in 2015 [77], who created a 3D environment by cross-linking fibrinogen (obtained from the BM supernatant of MM patients) with calcium and then carried out the culture by incorporating the remaining BM cellular components from MM patients, the encapsulation of the cells can also be accomplished using components from MM patients.

The previously mentioned cell cultures have the feature of being static 3D models in which the cells are encapsulated in materials made of extracellular matrix components or other proteins

that are present in *in vivo* models. However, because the hydrogel acts as a barrier to diffusion, the static condition reduces mass transfer, which is one of these model cultures' limitations.

To overcome this and other restrictions, and to offer new models that more closely resemble the *in vivo* environment in patients, tissue engineering focused on a 3D dynamic culture system based on the use of bioreactors. The dynamic culture condition allows, unlike static 3D cultures, for greater diffusion of gasses and nutrients and a non-air-liquid interface [78].

The Rotary Cell Culture System (RCCSTM) is one of the commercial bioreactors used in the development of 3D systems. This transparent, horizontally rotating device has no internal moving parts and eliminates any head space between the culture medium and atmosphere. By maintaining cells, spheroid cells or cellular aggregates in suspension with low shear, this system minimizes turbulence and shear forces that are typically associated with impeller-driven stirred bioreactors, as well as the risk of sedimentation and insufficient gas/nutrient supply [79], [80]. Furthermore, it also allows for adherent cells growth in a dynamic system with the help of microcarriers [80].

Ferrarini et al. used this platform in 2018 [78], and they found that the system could also maintain a well-preserved histo-architecture, including vessels and bone lamellae and vessels, for long-term culture using tissue from MM patients.

The 3D culture of adherent cells in the bioreactor was also carried out by Belloni et al. (2018) [61]. They used a gelatin scaffold into which they subsequently carried out the co-culture incorporating first primary pooled allogenic BMSCs and endothelial cells and then monoclonal PCs from MM patients.

In recent studies, researchers have developed three different 3D culture systems to mimic the bone marrow microenvironment for MM cells. Marin-Payà J.C. et al. created a biomimetic microgel made of alginate microspheres coated with BM ECM components. This system can be used as a disease model to test the effectiveness of antitumoral drugs by emulating the interaction between MM cells and the bone marrow ECM [53].

In another study conducted in 2022, a microgel culture system made of poly(ethyl acrylate) copolymers functionalized with ECM biomolecules, such as fibronectin, was developed. This platform can mimic both the bone marrow microenvironment by interacting with tumor cells and the CAM-DR effect generated by the biomolecules [81].

Additionally, Clara-Trujillo S. et al. designed a culture platform consisting of microspheres suspended in a semi-solid media (microgel) and coexisting with non-adherent MM cells growing dynamically in suspension. This system provides a three-dimensional dynamic context for MM cells and allows effective and selective presentation of bone marrow ECM molecules

to the cells. The microspheres can be modified with different functionalizations to further enhance the system's biomimicry [82].

All three culture systems are carried out under stirring, which improves the biomimicry of the system by conferring a dynamic character.

2. Aim of the study

In the previous chapter, we discussed the heterogeneity of MM disease and the importance of the microenvironment in disease progression and DR generation. We also presented the main MM 3D models available in the literature, which highlight the potential of tissue engineering to develop better biomimetic models. These models can provide platforms for studying DR processes with more clinically relevant conclusions, as they include different components of the BMN (BM resident cells, ECM components or both) whose influence on DR has been demonstrated in previous research.

To identify the involvement of different BMN components and their mechanism of action on tumor cells, it is helpful to have realistic disease models. In this work, we focus on studying a 3D culture platform that allows for the analysis of the interaction of MM cells with different ECM components. This model will enable us to identify the interaction of cells with each of the biomolecules of interest and study the involvement of each one in the generation of DR. This knowledge can contribute to the development of new drugs with specific targets.

Microspheres offer extensive versatility as 3D substrates, as well as the possibility of assembling a microenvironment of semi-solid nature, formed by suspended microspheres and cells, whose particle density can be fine-tuned. In addition, microspheres can be functionalized with biologically relevant molecules from the BM ECM to provide an *in vitro* platform able to test the role of these biomolecules in DR generation under biomimetic conditions. Furthermore, multiple myeloma cells (MMCs) and supporting microspheres can be deposited on conical agarose wells, which are permeable to water and soluble substances.

This thesis proposes the development of a biomimetic MM model for studying DR generation through tissue engineering techniques. To achieve this, the following considerations should be taken into account. First, a three-dimensional environment is essential to accurately replicate the native interactions of the BMN *in vitro*. Secondly, ensuring motility of MM cells is crucial. A more fluid model could enhance the diffusion of growth factors and cytokines and replicate indirect communication between cells and the ECM or between different types of cells.

Another important aspect to consider is that a 3D semi-solid model composed of suspended microspheres and unencapsulated cells could meet the aforementioned requirements.

Furthermore, incorporating various BM ECM biomolecules onto the surface of microspheres would improve the model's biomimicry and make it a useful tool for researching the roles played by different ECM constituents in the development of drug resistance. This model could

produce a simplified but physiologically meaningful representation of cell-ECM interactions and lead to an improved understanding of these interactions.

The aim of this work is to contribute to the development of a 3D culture platform for Multiple Myeloma tumor cells, in order to enable practical testing of antitumoral drugs.

The system will comprise of microspheres made of alginate that are suspended with MM cells. To enhance the biomimetic nature of the microspheres, active functionalization will be incorporated through the inclusion of proteins and glycosaminoglycans from the BM ECM

The MM1.S cell line will be employed to validate the platform as a 3D model for MM. Further, the RPMI8226 cell line will also be used to test DR generation in the presence of the different biomolecules of the ECM grafted onto the microspheres.

The specific objectives of the Thesis are:

- Synthesis of biomimetic microspheres (microgel) using a microfluidic system.
- Surface functionalization of microspheres using the Layer by Layer (LbL) technique, incorporating components of the ECM of the BM, such as CS, Hep, HA, and grafting of Col I onto the LbL-produced coating.
- Morphological and biochemical characterization of both the uncoated microspheres and their coatings.
- Experimental culture protocol to determine optimal cell culture conditions.
- Validation of the developed 3D culture platform, combining the fabricated and characterized biomimetic microgels with the co-culture of MMCs and human mesenchymal stem cells (hMSCs).
- Proliferation assay to study the effects of both components (microspheres and hMSCs) on MMCs.
- Utilization of the microgel 3D platform to investigate DR generation *in vitro* to dexamethasone.

3. Materials and Methods

3.1. Materials

Commercial extra virgin olive oil (La Masía), soy lecithin, sodium alginate from brown algae (Alg), calcium carbonate (CaCO_3), and acetic acid, all from Sigma-Aldrich, are used in the production of magnetic alginate microspheres (MO). The procedure also involves the use of Milli-Q water, iron oxide magnetic nanoparticles (Fe_3O_4 Ferrotec), 98% ethanol, and chloroform (Scharlab).

Poly-L-lysine hydrobromide, shark cartilage chondroitin sulfate, sodium salt of Streptococcus hyaluronic acid, heparin, N-hydroxysuccinimide (NHS), glycine (Gly), all from Sigma Aldrich, anhydrous calcium chloride (CaCl_2 PANREAC), and N-(3-dimethylaminopropyl)-N'-ethylcarbodiimide (EDC; Iris Biotech GmbH) are used for the functionalization of microspheres through layer-by-layer technique. Bovine Collagen I used for functionalizations is from PureCol, and glutaraldehyde (GA; Scharlab) is employed. For pH adjustment, chlorhydric acid (HCl) and sodium hydroxide (NaOH), both from Scharlab, are used.

Three commercial cell lines are employed in the cell cultures of this work: on one hand, the multiple myeloma cells MM.1S and RPMI8226 (American Type Culture Collection, ATCC), and on the other hand, human bone marrow mesenchymal stem cells (PromoCell, Heidelberg, Germany). The media used to culture all of them comprise Dulbecco's Modified Eagle Medium (DMEM), Roswell Park Memorial Institute Medium (RPMI) 1640 with and without phenol red (Sigma-Aldrich) and supplemented Mesenchymal Stem Cell Growth Medium 2 (Promocell). To supplement the media, fetal bovine serum (FBS) from Gibco, penicillin-streptomycin (P/S) (Fisher), trypsin-EDTA (Sigma-Aldrich), and L-glutamine (L-Glut) from Lonza are added. Also, as part of the platform or the steps to make the culture, Dulbecco's Phosphate-Buffered Saline (DPBS), Agarose (Sigma-Aldrich), 75 cm^2 adherent flasks (T75; SPL LIFE SCIENCES), 25 cm^2 non-adherent flasks (T25; FLASK), untreated p12 multiwell plates (FALCON), and Cytodex[®] 1 microcarrier beads (Sigma-Aldrich) are used in cell culture.

To determine the cell proliferation, the 3-(4,5-Dimethylthiazol-2-yl)-5-(3-carboxymethoxyphenyl)-2-(4-sulfophenyl)-2H-tetrazolium (MTS) assay kit (Abcam) is used. Also, the drug Dexamethasone (Sigma-Aldrich) is tested on the platform.

3.2. Microspheres' Production

Microspheres are produced by microfluidics. This technique is based on the immiscibility of 2 different liquids to obtain droplets of one of them. Both liquids flow, but one of them (the continuous media) breaks the other (the discontinuous media) into tiny spherical particles, the spheres. The device has a flow-focusing geometry with a 500 x 500 μm channel size and is made at the Centre of Biomaterials and Tissue Engineering with silicone. After their obtention, it is necessary to crosslink and collect them. All the assembly to produce the microspheres is shown in Figure 9.

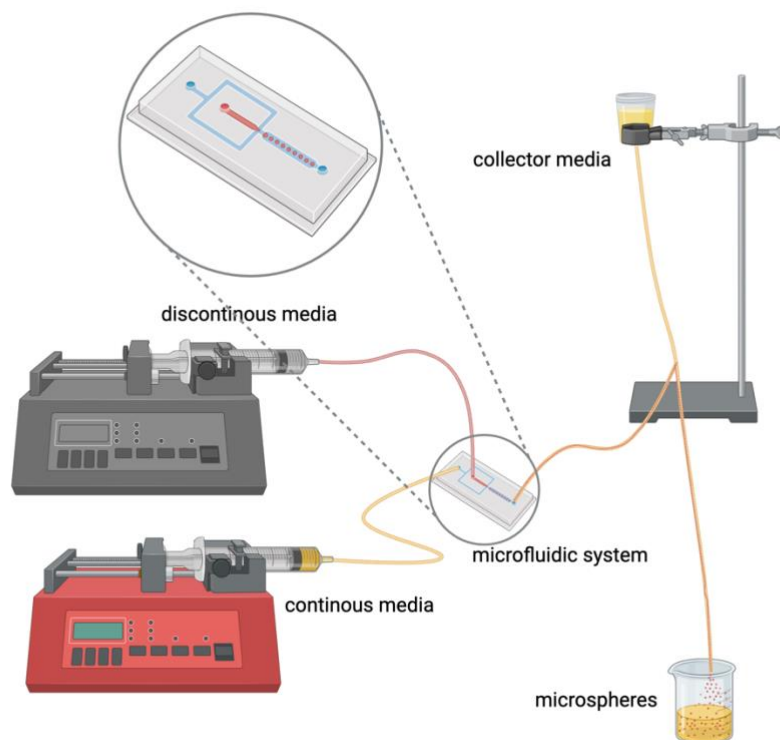


Figure 9. Assembly for the obtainment of microspheres with a close-up of the microfluidic system. Created with BioRender.com.

A 1.5% w/v alginate solution (Alg) in ultrapure water with 5% w/w_{ALG} of iron ferrite nanoparticles (Fe_3O_4) and 0.25M of calcium carbonate (CaCO_3) is used as a discontinuous media. The continuous media contains a 1% w/w_{OIL} soy lecithin and olive oil solution while the collector media has the same composition as the continuous media but with a 2% w/w acetic acid.

The pumps push the discontinuous and continuous media with a flow rate of 1.55 mL/h and 50 mL/h through the microfluidics device. This forms the alginate microdroplets, but they are not crosslinked till they do not arrive at the collector tube. There, the continuous and the collector

media merge and the acetic acid of the collector media decreases the pH, enabling the CaCO_3 dissociation which releases the calcium ions and ionically cross-links the microspheres.

When the synthesis is finished, it is necessary to remove the oil. To do it, chloroform was used to rinse the microspheres. After that, they were cleaned with ultra-pure water and preserved in 70% ethanol for storage.

3.3. Microspheres' Functionalization

For this study, the layer-by-layer (LbL) technique of immersive type is chosen to functionalize the microspheres [83] (Figure 10). This method involves adding alternating layers of biomolecules to the microspheres.

The alginate microsphere's negative surface charge is exploited to initiate coating with a polycation, Poly-L-Lysine (PLL). The next step involves managing different pairs of oppositely charged polyelectrolytes, which attract each other and consolidate the different layers to generate a six-layer thick coating. This coating presents biomolecules of interest from the ECM on its surface, including Hyaluronic Acid (HA), Heparin (Hep), Chondroitin Sulfate (CS), and Type I Collagen (Col I).

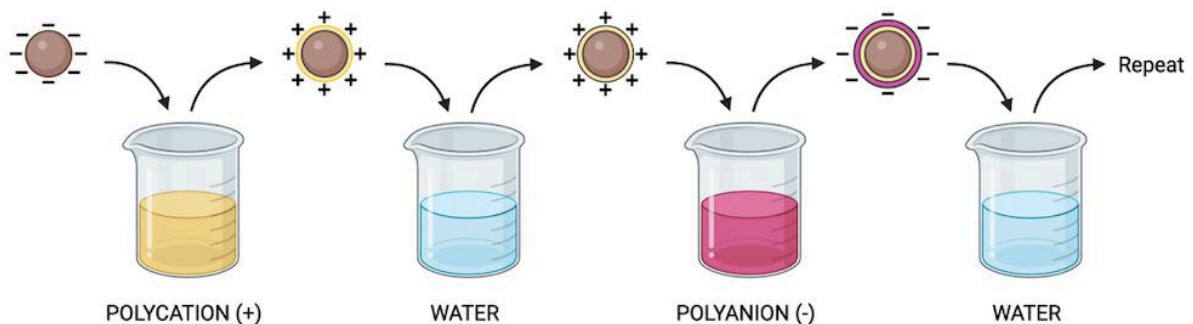


Figure 10. General scheme of the LbL process. Created with BioRender.com.

It is worth noting that the functionalization process is the same for the PLL/HA, PLL/CS, and PLL/Hep pairs since CS, HA, and Hep are polyanions. However, as Col I is positively charged, the process for its functionalization is different. Additionally, it should be emphasized that all functionalizations are carried out after autoclaving the microspheres, i.e., under sterile conditions, and using sterile or disinfected elements. Because of this, the solutions of polyelectrolytes were prepared and sterilized after adjusting their pH, by passing them through a PES filter with a syringe to eliminate contamination sources.

3.3.1. Layer-by-layer of Poly-L-Lysine and Chondroitin Sulfate

The process for these molecules involves coating the alginate microspheres (MO) with three layers of polyelectrolytes - PLL (positive) and CS (negative) - as shown in Figure 11. To ensure proper coverage on all microspheres, a PTR-35 rotational shaker (Grant-Bio) was used during all immersion and washing steps. This helps to minimize the formation of aggregates between microspheres and guarantees the correct coverage across the entire surface.

To prepare the LbL solutions, specific steps must be followed: first, the PLL solution at 0.05% w/v and 0.075M CaCl₂ is prepared by mixing 0.5 mg/mL of PLL in Milli-Q water and 0.07575 M CaCl₂. The solution must be homogenized for at least 1 hour. Next, the CS solution at 0.1% w/v and 0.075M CaCl₂ is prepared by mixing 1 mg/mL of CS in Milli-Q water and 0.075M CaCl₂. The solution must be homogenized for at least 1 hour. Then, the washing water is prepared by mixing 75 mM CaCl₂ in Milli-Q water.

For all the solutions, the pH needs to be adjusted to 7 using low molarity NaOH and HCl solutions.

Finally, the cross-linking solution is prepared by mixing 60 mM EDC, 30 mM NHS, and 75 mM CaCl₂ in Milli-Q water. This solution must be homogenized for at least 2 hours. There is no need to adjust the pH of this solution.

Before using these solutions for coating, they must be filtered with sterile 0.22 μm PES filters.

To start the functionalization process, the microspheres are recovered from the container where they were autoclaved. For this purpose, a sterile Pasteur pipette, a sterile 70 μm cell strainer, and a previously autoclaved silicone brush are used. Approximately 1 to 2 mL of microspheres should be recovered to maintain a controlled ratio of liquid to microspheres of approximately 10:1.5. Next, the microspheres are transferred to a 15 mL Falcon tube containing washing water. The tube is tightly sealed and needs to be rotated for 30 minutes.

The microspheres are conditioned and collected in the same manner as before, using the cell strainer, Pasteur pipette, and silicone brush. After removing the water, they are transferred to another 15 mL Falcon tube containing the filtered PLL solution. The tube is shaken on a rotational shaker for 10 minutes to ensure all microspheres come into contact with the solution. Afterward, the PLL is removed from the Falcon tube using a Pasteur pipette while retaining the magnetic microspheres with a niobium magnet, and the polyelectrolyte is reserved to use it in the next layers. The microspheres are then washed for 10 minutes to remove any remaining PLL residues.

Next, as a polyelectrolyte change is performed, the entire microsphere suspension is collected in a strainer, discarding the washing water. The microspheres are then transferred to another Falcon containing the CS solution and left to agitate for 10 minutes. Afterward, with the help of the magnet, the CS solution is removed and replaced with washing water, which cleans the microspheres for 10 minutes. This process is repeated two more times to obtain a total of three bilayers of PLL/CS coating.

After the final wash of the last bilayer, the MO is sieved once more and then transferred into a Falcon tube that contains the cross-linking solution of EDC/NHS. The microspheres are left submerged in this solution overnight with agitation, to uniformly cross-link all the microspheres. It is noteworthy that this chemistry generates covalent bonds between 1 carboxyl group (polyanion) and 1 amine group (polycation).

The next day, two 15-minute washes with washing water are performed to effectively remove the cross-linking solution. Finally, the microspheres are stored in Milli-Q water under sterile conditions in the refrigerator (4 °C) until it's time to use them.

To summarize the procedure, the scheme of the procedure is as follows: Washing water – PLL - Washing water – CS - Washing water – PLL - Washing water – CS - Washing water – PLL - Washing water – CS - Washing water - EDC/NHS - Washing water - Washing water.

3.3.2. Layer-by-layer of Poly-L-Lysine and Heparin

PLL/Hep LbL requires coating alginate microspheres with a total of three bilayers of the polyelectrolytes poly-L-lysine (positive) and heparin (negative). Solutions of PLL, Hep, washing water, and the cross-linking solution EDC/NHS must be prepared in order to accomplish this. The concentrations are the same as those used in PLL/CS, replacing the CS solution with Hep and adjusting the pH to 5.5.

Just as with PLL/CS, the process used for PLL/Hep LbL is the same. Therefore, the general scheme of the procedure is: Washing water – PLL - Washing water-Hep - Washing water – PLL - Washing water - Hep-Washing water – PLL - Washing water – Hep - Washing water - EDC/NHS - Washing water - Washing water.

3.3.3. Layer-by-layer of Poly-L-Lysine and Hyaluronic Acid

PLL/HA LbL requires coating alginate microspheres with a total of three bilayers of the polyelectrolytes poly-L-lysine (positive) and hyaluronic acid (negative). Solutions of PLL, HA, washing water, and the cross-linking solution EDC/NHS must be prepared in order to accomplish this. The concentrations are the same as those used in PLL/CS, replacing the CS solution with HA and adjusting the pH to 5.5.

Just as with PLL/CS and PLL/Hep, the process used for PLL/HA LbL is the same. Therefore, the general scheme of the procedure is: Washing water – PLL - Washing water - Hep-Washing water – PLL - Washing water - Hep-Washing water – PLL - Washing water – Hep - Washing water - EDC/NHS - Washing water - Washing water.

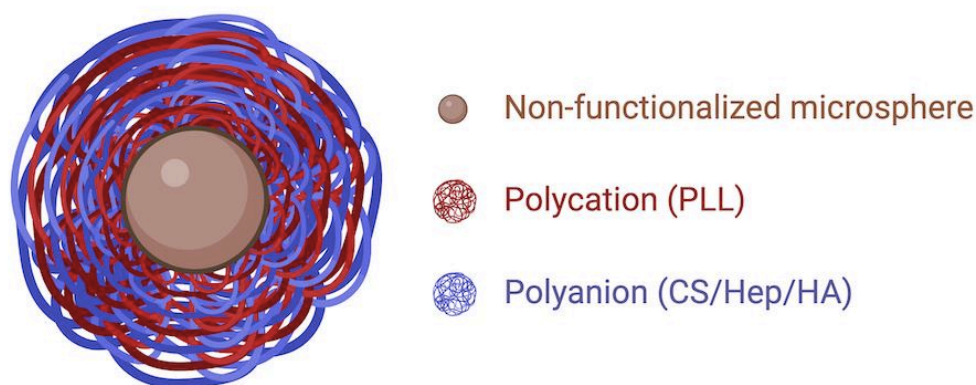


Figure 11. Functionalized microsphere through the layer-by-layer technique with a polycation (PLL) and a polyanion (CS/Hep/HA). Created with BioRender.com.

3.3.4. Grafting of Type I Collagen

Col I grafting requires coating the microspheres with two and a half bilayers: two complete PLL/CS bilayers and a final layer made entirely of PLL. To these layers, a collagen I graft is then applied (Figure 12). In order to do this, the same PLL, CS, and washing water solutions as in the PLL/CS Lbl, at the same concentrations and pH, are prepared. Furthermore, solutions of glutaraldehyde (GA), collagen I, and glycine (Gly) must be prepared.

To prepare the GA solution, the stock of GA with a 25% purity is diluted to 0.5% w/v in Milli-Q water. The Gly solution consists of 0.2 M glycine in Milli-Q water and is stirred for 20 minutes.

Both solutions must be prepared on the same day of use and filtered with a pre-filtered PES filter. The commercial sterile Col I 3 mg/mL solution is diluted to obtain the collagen I solution

at 1 mg/mL. To achieve this, and to maintain the characteristic acidic pH of collagen I, "acidic water" is used. It consists of washing water with 0.2 M acetic acid. This acidic water is then filtered, and the appropriate volumes of Col I 3 mg/mL and acidic water are mixed in a sterile manner to obtain the desired final concentration of 1 mg/mL.

Up until two and a half bilayers – that are, two PLL/CS bilayers and a final PLL layer – the coating procedure is the same as PLL/CS LbL. Following the last layer and its corresponding wash, the microspheres are placed in a closed container with the GA solution and left to stir for 1 hour. After that, the microspheres are sieved, getting rid of the GA, and recovered in a new container with washing water for 10 minutes. To effectively remove any unbound GA from the microspheres, a second wash with water is performed for another 10 minutes. Next, the microspheres are transferred to a Falcon tube containing the Col I solution and left to stir overnight in the bioreactor. In this coating, the collagen and the PLL are crosslinked to each other because one of the aldehyde groups of the GA bonds to an amino group of PLL and leaves the other exposed to bond Col I in the overnight step.

The collagen I solution is removed the following day, and the microspheres are twice washed with washing water for 10 minutes. The glycine solution is added to the microspheres after the washes and let it stir overnight. By taking this step, any unreacted aldehyde radicals from GA that may remain are inactivated, protecting cells from GA cytotoxicity.

The following day, the Gly solution is removed, and the microspheres are washed two consecutive times with washing water with orbital agitation. The microspheres are then transferred to a Falcon tube containing Milli-Q water and stored at 4°C under sterile conditions until their use.

The scheme of the procedure is as follows: Washing water – PLL - Washing water – CS - Washing water – PLL - Washing water – CS - Washing water – PLL - Washing water – GA - Washing water – Col I – Washing water - Gly - Washing water - Washing water.

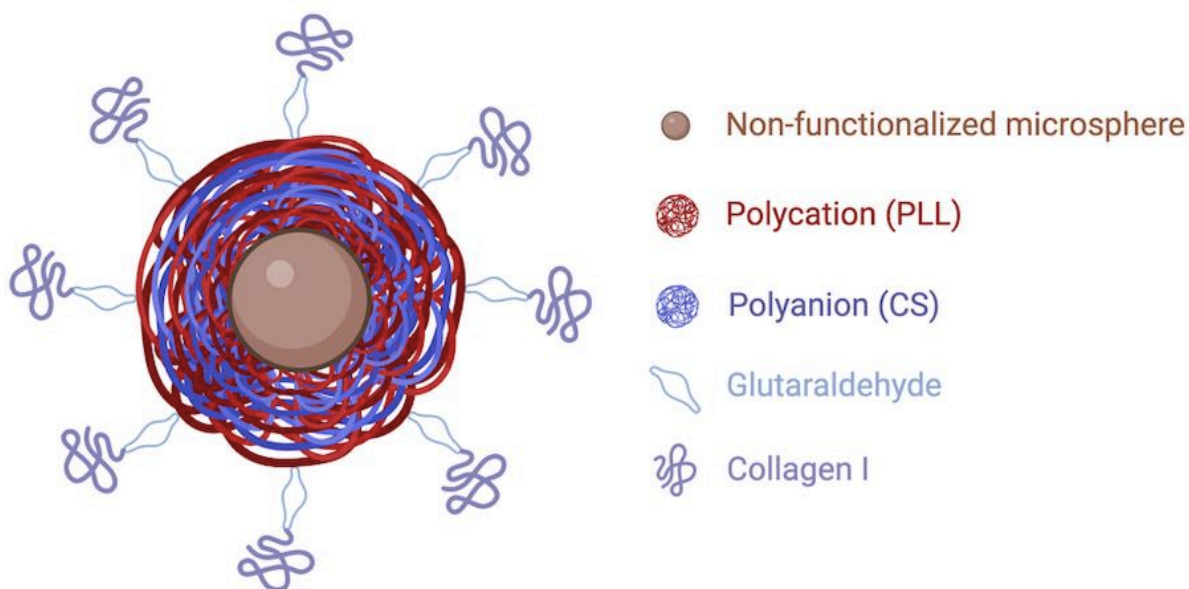


Figure 12. Functionalized microsphere through the layer-by-layer technique with the polycation PLL and the polyanion CS, and the final layer of Col I through the GA. Created with BioRender.com

3.4. Morphological Characterization: Optical Microscopy

To observe the microspheres' diameter, shape, and size distribution the inverted optical microscope Nikon Eclipse TS100-F, equipped with a camera, is used.

The process for staining the microspheres involves using the Alcian blue protocol. To prepare the Alcian blue solution, it is necessary to filter it through a filter paper to remove any dust, fibers, or sedimented salts or components. A Falcon tube is used to hold 1 mL of the Alcian blue solution, which is then mixed with 9 mL of Milli-Q water. The microspheres are added to the Falcon tube containing the diluted Alcian blue solution, and the tube is placed in a shaker with low RPMs for at least 30 minutes. After the microspheres have been stained, the Alcian blue solution is removed and replaced with water for a 5-minute washing period. This washing process is then repeated one more time.

For image capture, the microspheres are embedded in water and placed on a smooth surface. Once the images have been obtained, the microspheres' diameter is measured using the "ImageJ" software going through several steps. First, the desired scale (100 μm) is established. Subsequently, the image is converted into grayscale and then transformed into black and white by applying the Threshold function. The Watershed tool is then used to separate the spheres that are still partially connected. Finally, the microspheres of interest are selected and analyzed using the Analyze Particles function, which requires setting a minimum size limit for particles to be counted. Since the microsphere shape is not perfectly spherical, the Feret diameter, which gives a more realistic value for the diameters, is used. The data are then transferred to Excel to conduct additional analysis.

3.5. Biochemical Characterization of Microspheres and their Functionalization

Thermogravimetric Analysis (TGA) is used to detect the presence of biomolecules in the coatings in a non-specific manner.

3.5.1. Sample Preparation

After resuspending properly the microspheres in the Falcon tubes with a 1 mL pipette, one sample of each type (PLL/CS LbL, PLL/Hep LbL, PLL/HA LbL, Col I LbL and non-functionalized) is withdrawn and transferred into 5 labeled Eppendorf tubes. After that, each microsphere sample was placed in an alumina crucible and, with the help of a magnet, the Milli-Q water was removed from the crucible until reaching 10 mg of microspheres.

Powdered forms of alginate, PLL, HA, CS, and Hep are also subjected to TGA analysis. The collagen solution employed for coating is initially dried, and subsequently, the resulting powder undergoes analysis.

3.5.2. Thermogravimetric Analysis

Thermogravimetric analysis (TGA) is defined as a thermoanalytical technique that monitors the loss and/or gain of sample mass as a function of time or temperature. It determines the thermal stability of a compound and the fraction of volatile components it contains. It is used to validate the formation of coatings on particles' surfaces. To do this, thermogravimetry weights the sample while heating it steadily at a constant rate, allowing measures with great sensitivity (10⁻⁶ g). Volatile molecules of the components are released during the heating scan when heating values exceed the thermal energies of the different chemical bonds in the molecules. This causes a decrease in the mass of the molecule. To prevent outside factors from interfering with the weight measurement – most notably, combustion of airborne oxygen – the microbalance is housed in a chamber where the apparatus can produce inert gas atmospheres, like nitrogen, helium, or argon [84], [85].

The following parameters are set on the computer associated with the TGA equipment (Thermal Analysis Excellence TGA/DSC 2, Mettler Toledo): heating rate of 10°C/minute and nitrogen flow of 50 mL/minute. Samples with an initial weight of approximately 55 mg have been used. In the current work, this method is used to demonstrate that the coating does, in fact, consist of a portion of the PLL/CS LbL, PLL/Hep Lbl, PLL/HA LbL and Col I LbL microspheres. For

this reason, the functionalized microspheres' weight derivatives (normalized to dry weight) in relation to temperature have been compared to those of the uncoated, non-functionalized microspheres.

3.5.3. Data Analysis

The TGA microbalance records weight and temperature weight derivative changes as a function of temperature.

To examine the degradation and their derivatives, an Excel sheet has been generated. Normalizing the derivative by the sample's dry weight – that is, the weight left over after all the water has evaporated – is also required. It is noted that between 200 and 400°C, alginate shows a distinctive degradation that can be modeled using the sum of two normal curves. Consequently, to make the comparison, two normal curves that, when added together, represent the derivative curve of weight/temperature in each LbL series, have been generated. Finding variation from the alginate curve is the aim.

3.6. Cell Culture

Various cell cultures are established to address specific objectives. Initially, a culture protocol experiment is conducted to assess cell proliferation under both 2D and 3D conditions, considering the type and quantity of the culture medium. Subsequently, the platform is validated using different culture conditions and materials. Finally, drug testing is implemented to evaluate the impact of drugs on MMCs.

3.6.1. Culture Well Fabrication

A permeable culture support that permits direct and indirect exchange of soluble factors between hMSCs and MMCs is required for the development of a static culture. Furthermore, the wells on this support must have the right volume to hold both microgels, MMCs, and hMSCs pellets. For this reason, cubic hydrogels with four conical wells each have been developed as a platform for culture. The conical shape of microwells improves oxygen and medium delivery to cell aggregates, allowing for better fluid circulation, which makes it a better choice for 3D cell cultures than cubical or cylindrical microwells [86], [87].

Due to their dimension, each microwell can contain a total volume of 120 μL , of which the microgel occupies 7% v/v (based on Marin-Payà J. C. et al. work [81]). It is important to note that the microwell cannot be filled to the top, as the cells may spill out, resulting in a loss.

A 1.5% w/v agarose solution in Milli-Q water is used to make the culture supports. The solution must be autoclaved before its use. Agarose is selected due to its physical cross-linking properties, without the need to add chemical reactions to the process. Therefore, the support takes shape using different molds fabricated by Centre for Biomaterials and Tissue Engineering (CBIT) staff (Joaquín Ródenas Rochina, María Inmaculada García Briega, and Luís Amaro Martins).

The agarose solution is heated and poured into a cubic-shaped silicone mold, placed on a surface at a temperature lower than 4°C, thanks to which can cross-link. Another mold made of resin, which presents the negative of the four conical microwells where cell culture takes place, is positioned on top of the cubic mold. The entire cultivation platform can cross-link in less than 10 minutes thanks to the cold environment. After this, the cube is demolded and stored in sterile DPBS at 4°C until needed.

3.6.2. Cell Lines

To carry out the cell culture, cells from the multiple myeloma cell lines MM.1S and RPMI8226 (MM) are used. For the co-culture, two types of cells are used: MM.1S or RPMI8226 cells and human mesenchymal stem cells (hMSCs). MM.1S and RPMI8226 cells are cultured in suspension while the hMSCs, which are adherent cells, are cultured in contact with a surface. In this work, Cytodex[®] 1 microspheres, which are adherent microcarriers, are used to carry out the culture hMSCs in a pellet.

3.6.3. Thawing and Expansion of cells

To prevent contaminations, all materials, media, tubes, vials, hydrogels, and cells that will be used in the culture must be handled as aseptically as possible. This requires working exclusively in laminar flow hoods, disinfecting as needed with 70% ethanol, and using sterile or autoclaved consumables.

Preparation of culture media:

- Complete DMEM, composed of DMEM medium (89% v/v), FBS (10% v/v) and P/S (1% v/v). Used in the thawing of hMSCs.
- Complete Promocell, composed of Mesenchymal Stem Cell Growth Medium 2 (89% v/v), its supplement (10% v/v) and P/S (1% v/v). Used in the thawing and expansion of hMSCs and for manufacturing of hMSC pellets.

- Complete RPMI, composed of RPMI 1640 with phenol red (88% v/v), FBS (10% v/v), L-glutamine (1% v/v) and P/S (1% v/v). Used in the thawing and expansion of MMCs.
- Complete RPMI without phenol red, composed of RPMI 1640 without phenol red (88% v/v), FBS (10% v/v), L-glutamine (1% v/v) and P/S (1% v/v). Used in the culture to prevent interference by phenol red with the MTS assay.
- Complete RPMI with a higher concentration of glucose, composed of RPMI 1640 with 10 mM Hepes, 1mM sodium pyruvate, and 4.5 g/L of glucose (88% v/v), FBS (10% v/v), L-glutamine (1% v/v) and P/S (1% v/v). Used in the culture protocol experiment.

All solutions are filtered with sterile PES filters to ensure sterility.

3.6.3.1. Thawing and expansion of hMSCs

On day -7 of cell culture, hMSCs need to be thawed and expanded. To accomplish this, a cryotube containing 1 million hMSCs in 1 mL of FBS with 10% dimethyl sulfoxide (DMSO) is extracted from liquid nitrogen, in which is frozen. After the content of the cryotube is thawed in a 37 °C water bath for 1 minute, the cells are resuspended in 9 mL of complete DMEM medium to inactivate the DMSO (thanks to the FBS). The suspension is subsequently centrifuged at 250 G for 5 minutes. The supernatant is decanted, and the pellet is resuspended in 1 mL of complete Promocell medium. Cell counting is performed using a Neubauer chamber, and the cells are seeded at a density of 300,000 cells/flask (T75 adherent) in a final volume of 10 mL. After a washing with PBS, the cells are expanded for 4 days in the incubator, changing the 10 mL of medium with fresh one on day -5 of culture. Since these cells are not going to be used for differentiation assays, a maximum of 80% confluence is reached, at which point they are either used for seeding on Cytodex 1 or subcultured to continue their expansion.

On day -3 of culture, hMSC pellets need to be prepared, as they will be seeded along with MMCs. Cryotubes with perforated caps are used for this purpose because they allow proper oxygenation of hMSCs and because they provide pellet formation thanks to their conical shape. The pellets consist of 300 µL of complete Promocell medium containing 60,000 hMSCs and 3 µL of adherent Cytodex microspheres that were previously conditioned in complete Promocell medium. Every 30 minutes for a total of 5 times, manual resuspension is carried out with the use of a pipette to ensure the proper distribution of spheres and cells. At that point, after 30 more minutes from the last homogenization, 300 µL of additional expansion medium is added, resulting in a final volume of 600 µL, and it is left to rest for 72 hours to complete pellet formation.

3.6.3.2. Thawing and Expansion of MMCs

5 million multiple myeloma cells are thawed from a cryotube with 1 mL of medium containing 5% DMSO on day -5 of culture. After the cryotube is placed in a water bath at 37°C for one minute, the cells are rapidly resuspended and transferred to a Falcon tube with 9 mL of complete RPMI medium. The FBS in this medium inactivates the DMSO. The tube is then centrifuged at 250 G for 5 minutes, the supernatant is decanted and 4 mL of complete RPMI medium is used to resuspend the MMC pellet. These steps must be carried out quickly to avoid compromising cell viability since the cryopreservation medium contains 10% v/v DMSO, which is toxic at room temperature.

Once in a medium without toxic components, the cells are counted using a Neubauer chamber and seeded at a rate of 10 million cells/flask in a non-adherent T75 flask (used in a vertical position) with a final volume of 20 mL. The flask is left to incubate in an incubator with an atmosphere of 5% CO₂ and a temperature of 37°C to let the cells grow for 3 days. Every two days of culture, the medium is replaced with a fresh one.

3.6.4. Culture to Set the Operating Conditions

3.6.4.1. Experiment Setup

During the culture, cells consume the nutrients present in the environment at a particular rate. Every cell line has its rate and, moreover, the *in vitro* platform, the number of cells present in the medium, and other factors have an impact on this consumption rate. To reach the best proliferation outputs in the platform developed in this work, it is necessary to monitor this process closely, as it can significantly affect the outcome of the MM1.S cell line.

The focus of this experiment is to determine which glucose concentration is better for MM1.S cell line proliferation, checking the two most common (2 g/L and 4.5 g/L). It is also relevant to know if the presence of the soluble factors has a key role in their proliferation in the hydrogel. As the hydrogel allows the complete medium renewal or just half of it, both options are tested for both media compositions.

Four hydrogels are placed in individual wells of a p12 plate for seeding the cells. A micropipette is employed to remove any remaining DPBS residues from the plate's wells and the hydrogels' microwells. In addition, since it will be used throughout the cell culture, RPMI complete medium without phenol red (normal medium) and complete RPMI with a higher concentration of glucose (super medium) need to be prepared.

MMCs are cultured in 2D and 3D conditions. The 2D conditions consist of seeding the cells at a concentration of 60,000 cells/100 μ L of medium (complete RPMI medium) in four Eppendorf tubes and four wells of a p96 plate. Every two days of culture, the medium is replaced with a fresh one. The 3D conditions consist of seeding the cells at a concentration of 60,000 cells/100 μ L of medium in each microwell of four hydrogels. The 3D culture is performed with the two different media mentioned above.

To summarize, the conditions are:

- 3D condition with super medium (3D – SM): involves a suspension of MMCs in the hydrogel's microwells with super medium and a complete replacement of medium every two days.
- 3D condition with half change of super medium (3D – $\frac{1}{2}$ SM): involves a suspension of MMCs in the hydrogel's microwells in super medium and a half replacement of medium every two days.
- 3D condition with normal medium (3D – NM): involves a suspension of MMCs in the hydrogel's microwells with normal medium and a complete replacement of medium every two days.
- 3D condition with half change of normal medium (3D – $\frac{1}{2}$ NM): involves a suspension of MMCs in the hydrogel's microwells in normal medium and a half replacement of medium every two days.
- Multiwell plate condition (2D – P): involves a suspension of MMCs in four wells of a p96 plate.
- Eppendorf tube condition (2D – T): involves a suspension of MMCs in four Eppendorf tubes.

3.6.4.2. Trypan Blue Assay

Cell number is determined by Trypan Blue assay performed on days 3, 5, and 7 from seeding. It is a method based on the principle that live, healthy cells have intact cell membranes that exclude specific dyes, while damaged or dead cells have compromised membranes that allow the dye to enter and stain them.

To collect the cells, a small aliquot of the cell suspension is mixed with an equal volume of Trypan Blue solution. After collecting the cells, they are quantified using a Neubauer chamber and the counting is conducted under the optical microscope within the defined grid squares. A minimum of 50 cells were counted per replicate.

The number of cells is determined using the following formula:

$$\text{Number of cells} = \text{average number of cells in one large square} \cdot D_f \cdot FV \cdot 10^4$$

D_f = dilution factor

FV = final volume in which the cells are resuspended

GraphPad is used to analyze the data.

3.6.5. Culture for the Validation of the Platform

3.6.5.1. Experiment Setup

For the seeding, the hydrogels are placed in wells of p12 plates as shown in Figure 13. Two plates are used for five conditions, one for the two culture conditions with only MMCs and one for the three co-culture conditions with MMCs and hMSCs. A micropipette is used to remove any remaining DPBS residues from the plate's wells and the hydrogels' microwells. In addition, since it will be used throughout the cell culture, RPMI complete medium without phenol red needs to be prepared.

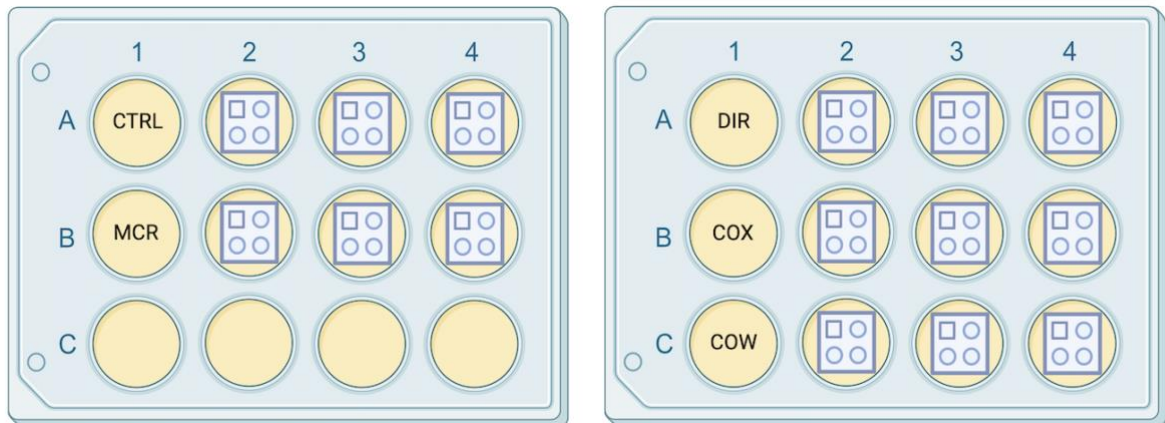


Figure 13. Hydrogels in p12 plates for cell culture. Created with BioRender.com.

Different cell culture conditions for MM.1S cells are carried out (Figure 14):

- Control condition (CTRL): consists of a suspension of MMCs in the hydrogel's microwells.
- Monoculture condition (MCR): suspension of MMCs along with the microgel in the same hydrogel's microwell.
- Direct co-culture condition (DIR): suspension of MMCs and hMSC pellets in the same hydrogel's microwell.

- Indirect co-culture condition without microgel (COX): suspension of MMCs in the hydrogel's microwell along with the hMSC pellet outside the hydrogel.
- Indirect co-culture condition with microgel (COW): suspension of MMCs along with the microgel in the same microwell and the hMSC pellet outside the hydrogel.

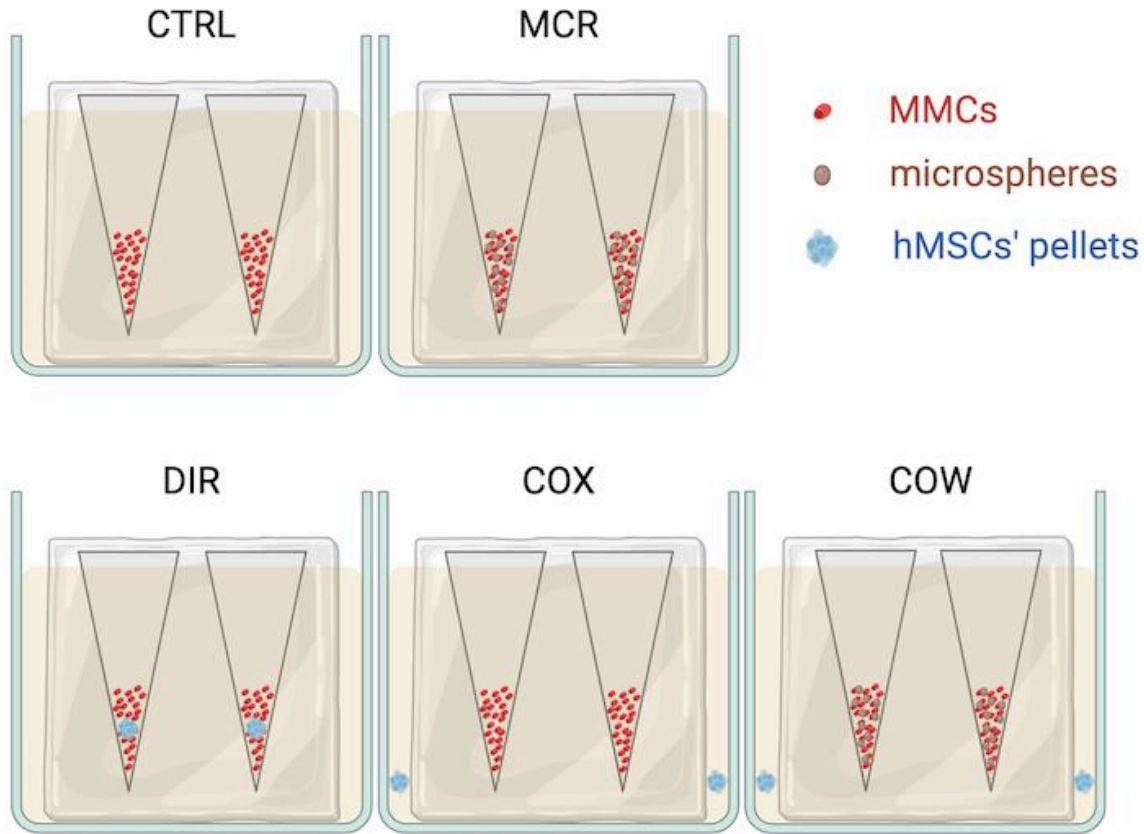


Figure 14. Illustration of the cell culture in the hydrogels' conic microwells showing the 5 different conditions: CTRL, MCR, DIR, COX, and COW. Created with BioRender.com.

The first step in creating the conditions with microgel is to transfer the appropriate volume of microspheres to the microwell. To incorporate them, a suspension of microspheres of all types properly mixed is made, with a 25% proportion of each kind. The total number of microwells is considered when calculating the total amount of microspheres to be added, and the portion of the microwell that they occupy equals 7% of the total microwell volume, corresponding to 8.4 μL in this case. After taking separately each type of microspheres, they are combined with the mixed solution, and 8.5 μL of the mixture is added into each microwell.

For the conditions in which there is a co-culture, the hMSC pellets need to be transferred using a pipette with cut tips (in order to not break the pellets). In the case of indirect co-cultures, the pellets are transferred to the well of the plate outside the hydrogel, adding one pellet for each well of the hydrogel containing MMCs. Direct co-culture involves transferring the pellets directly to the microwell that contains MMCs (one pellet in each microwell of the hydrogel).

Plasma cells must be added in all conditions, regardless of the other components. To accomplish this, MMCs are recovered from the flask in the incubator, centrifuged at 250 G for 5 minutes, and then counted using a Neubauer chamber. After the number of cells is determined, the required cells are prepared at a concentration of 60,000 cells/100 μ L of medium and seeded into each of the microwells of all the hydrogels. It is fundamental to underline that the ratio of hMSCs to MMCs seeded should be around 1:1. For this reason, each hydrogel contains 4 pellets of 60,000 mesenchymal cells (inside or outside the microwells, depending on the condition) and 60,000 myeloma cells in each microwell.

In conclusion, approximately 1.5 mL per well of complete RPMI medium is used to fill the volume of the well outside the hydrogel. To prevent medium evaporation, empty wells of the plate are filled with 1 mL of sterile DPBS/MilliQ H₂O.

3.6.5.2. MTS Assay

Cell proliferation is determined by colorimetric MTS assay performed on days 3, 5, and 7 from seeding in the agarose microwells. It is a colorimetric assay that allows the estimation of viable cells, which is proportional to the absorbance of the resulting-colored reagent. The reaction is based on the reduction of the MTS reagent (3-(4,5-dimethylthiazol-2-yl)-5-(3-carboxymethoxyphenyl)-2-(4-sulfophenyl)-2H-tetrazolium) to formazan (colored compound) due to the activity of the NAD(P)H-dependent dehydrogenase enzyme. The reagent changes color because of its reduction by cellular metabolism. Therefore, the assay only detects viable cells, as non-viable cells do not exhibit enzymatic activity.

After carefully homogenizing the contents of the microwell for samples without microgels or direct co-culture, the cells of CTRL and COX conditions are transferred to the appropriate Eppendorf tube. The caps of the tubes are pierced to ensure proper gas diffusion because the cells will be in the tubes for a while.

To guarantee the proper cell collection, the microwell is washed three times with 100 μ L of DPBS, homogenizing the content before transferring it to the Eppendorf tube. In addition, the microwells are checked under an optical microscope to make sure no cells are left inside; if any are, further DPBS washes are carried out as necessary.

To be able to properly collect the hMSCs pellets from the microwell for samples from direct co-culture (DIR), micropipette tips with cut ends are used. It is important to collect the sample without homogenizing otherwise, the pellets could break and hMSCs could mix with MMCs.

The content of the microwell is transferred to the corresponding Eppendorf tube, passing through a 70 μL filter to retain the pellet and allow the cells to pass. In this instance, the microwell is cleaned with 3 DPBS washes before being examined under the optical microscope to ensure that no MMCs are left inside.

For microgel samples (MCR and COW), the content of the microwell is homogenized and collected using also cut micropipette tips to facilitate the collection of functionalized microspheres. The content is transferred to an intermediate Eppendorf tube that has been sterilized and placed next to the magnet. This Eppendorf's content is properly homogenized to allow the detachment of the MMCs from the microspheres. The magnet then retains the MO in place while the MMCs are moved to the Eppendorf with the perforated cap. To retain the MO and recover all the cells, this last step is repeated three times washing with DPBS.

After collecting the cells, in the Eppendorf tubes, they are centrifuged at 250 G for 5 minutes and then resuspended in 250 μL of complete RPMI without phenol red medium per Eppendorf. Simultaneously, a calibration curve using MMCs is prepared. To accomplish this, the necessary cells are taken from the T25 flask where the remaining seeding cells are still growing. Three biological replicates of the required cells are made for each point on the curve. For each condition, cell culture medium without cells is used as a blank.

25 μL of MTS reagent is added to the cells from the samples and the calibration curve, which are in the Eppendorf tubes with 250 μL of complete RPMI medium without phenol red. They are then placed in the incubator for 1 hour and a half. Following this time, the tubes are centrifuged, and the resulting supernatant is removed and two technical replicates for each biological replicate (BR) are placed in a p96 multiwell plate, which is read at 490 nm on the Perkin Elmer Victor X3 Multilabel Plate Reader spectrophotometer.

The absorbance data obtained from this analysis are processed in Excel and correlated with the number of cells. In the end, GraphPad is used to analyze significant differences between populations.

To better understand the cell culture and MTS assay timelines, a temporal scheme is provided in Figure 15.

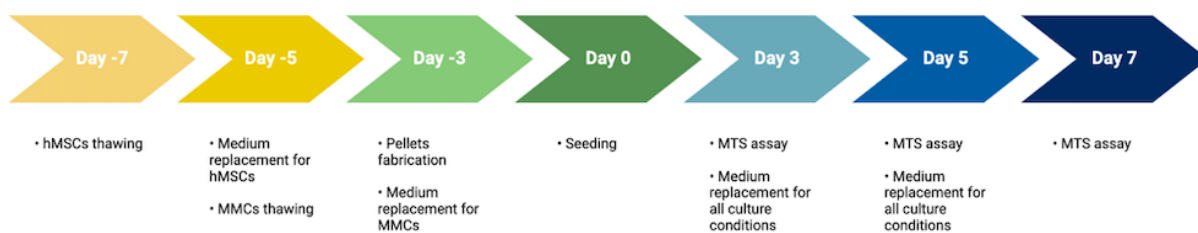


Figure 15. Cell culture for the validation of the platform timeline.

3.7. Drug Resistance Analysis

Cells are exposed to 1 μ M Dexamethasone (DEX) for 72 hours. In addition, a control without drugs is prepared and used to normalize each of the condition viability results.

An MTS assay is performed to determine cell proliferation and the data are processed in Excel and then analyzed using GraphPad.

3.8. Statistical analysis

After obtaining the data from any of the assays that have been carried out, GraphPad is used for an initial analysis to identify and, when present, remove outliers. Any anomalous data is then discarded using the ROUT method with a $Q=5\%$. Excel is used for the analysis of the characterization data, with the results shown as the mean \pm standard deviation.

The GraphPad tool is used to perform the data analysis related to cell culture. Anomalous values are eliminated and then the data are subjected to a normality analysis using the Shapiro-Wilk test. Parametric tests like one-way ANOVA, which compares differences with respect to a single variable, and two-way ANOVA, which compares differences with respect to multiple variables, are performed if the data are normal. The Brown-Forsythe correction is used if it is not possible to assume that the standard deviations (SDs) are equivalent. If they are equal, ANOVA is used without correction.

If a normal sample's p-value is at least 0.05, then the differences between groups are considered statistically significant. Significant differences are indicated by the symbols * ($p \leq 0.05$), ** ($p \leq 0.01$), *** ($p \leq 0.001$), and **** ($p \leq 0.0001$). Insignificant differences are indicated by the symbol "ns" or left blank ($p \geq 0.05$). Significant differences are indicated by the number # if the samples fail the normalcy test.

4. Results and Discussion

The overall result of this work is the development of a three-dimensional environment in which MMCs can be cultured to assess the effect of different drugs on MM development. For this reason, creating an *in vitro* culture platform that allows for the recreation of the biological niche in which MM develops is the focus. To achieve this, functionalized alginate magnetic microspheres, that present extracellular matrix biomolecules, are fabricated to simulate the acellular component of the niche, and hMSCs are employed as the cellular component. In this way, it is intended that the platform can resemble what occurs *in vivo*. The microspheres are examined and characterized morphologically and biochemically through different techniques and assays, and the platform is tested by performing various cell cultures and their corresponding cell proliferation assays.

4.1. Morphological Characterization of Magnetic Microspheres: Size Distribution

As mentioned in section 3.2., a silicone microfluidic system (Figure 9) based on the dispersion of an aqueous phase into a lipidic phase has been used to fabricate microspheres. Due to the principles of microfluidics, the flow parameters of continuous and discontinuous media, which modulate the diameter of the particles produced, are crucial to the characteristics of the microspheres employed in this work. Using one of the synthesized samples as a representation of the process and measuring the diameter of around 50 of them, an average size of $126 \pm 35 \mu\text{m}$ is obtained.

As shown in Figure 16_A, the synthesis of the microspheres through microfluidics enables the acquisition of a normal-size distribution. Furthermore, the majority of the obtained microspheres exhibit a diameter between 98 and 130 μm . The brown color of the microspheres and the absence of iron ferrite aggregates within them serve as additional indicators of the uniform dispersion of iron ferrite nanoparticles (Figure 16_B). This confirms that the selected method of nanoparticle dispersion is effective.

The coating process involves immersing the microspheres initially in a polycation (PLL) solution, followed by a polyanion (CS/Hep/HA) solution, and repeating these steps twice. Subsequently, the coating undergoes cross-linking using an EDC/NHS solution. Notably, the functionalization process for Col I, which is positively charged, differs: after two layers of PLL/CS and a final layer of PLL, the samples are immersed in a GA solution and, finally, in a Col I solution.

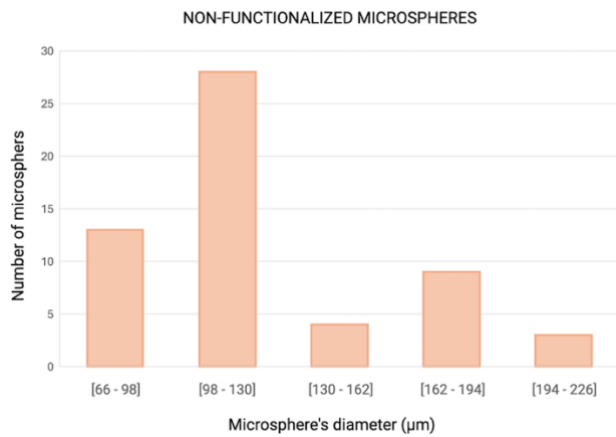
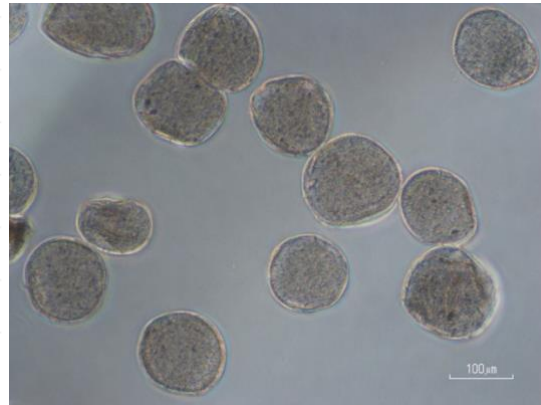
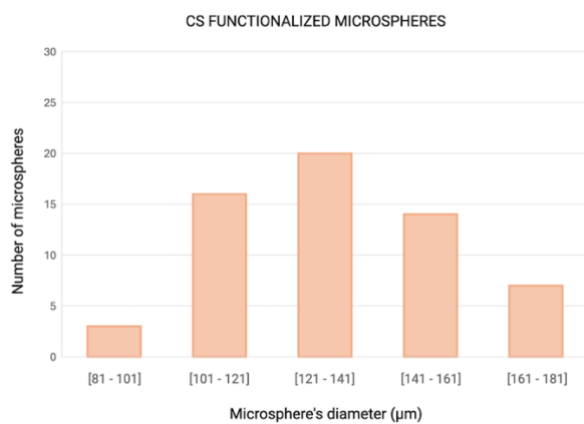
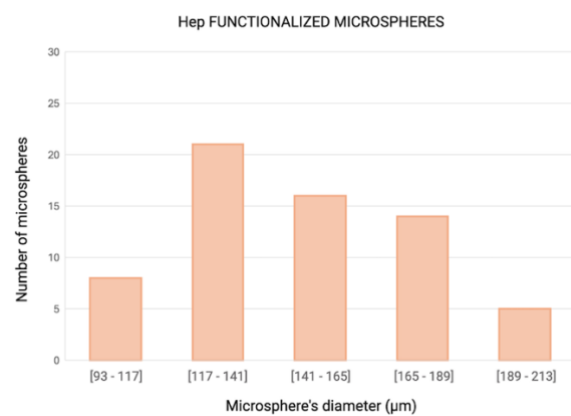
A**B**

Figure 16. A) Diameter distribution of non-functionalized alginate microspheres with ferrite. B) Microspheres observed under an inverted microscope on a scale of 100 μm .

In Figure 17, the diameter distribution of the microspheres with different types of functionalization (CS, Hep, HA, and Col I) is shown. It can be observed that the microspheres have a $136 \pm 22 \mu\text{m}$ average diameter size in the case of CS functionalization (Figure 17_A), while for Hep functionalization is $149 \pm 27 \mu\text{m}$ (Figure 17_B). For HA functionalization the average size is $137 \pm 21 \mu\text{m}$ (Figure 17_C), and $130 \pm 20 \mu\text{m}$ for Col I functionalization (Figure 17_D).

Given that microspheres of this size have been successfully tested in culture previously [88], the obtained size is appropriate for the upcoming use of these microspheres as a biomimetic environment in multiple myeloma.

A**B**

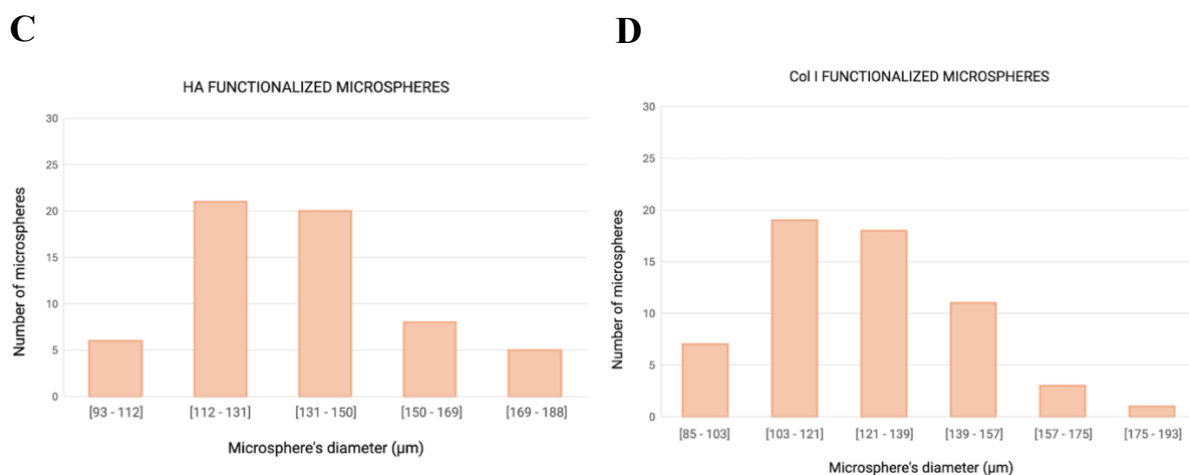


Figure 17. Diameter distribution of alginate microspheres functionalized with CS (A), Hep (B), HA (C), and Col I (D).

4.2. Biochemical Characterization of Magnetic Microspheres: TGA

TGA was employed to investigate the thermal stability of microspheres functionalized with the different types of LbL coatings (PLL/CS, PLL/Hep, PLL/HA, Col I) described in section 3.3. The temperature at which each chemical bond of the polysaccharide or protein chain is broken in a heating scan is a characteristic value that helps to identify and quantify the fraction in which a given molecular group is present in the sample composition. In our case, we use the technique to determine the mass fraction of the coating deposited on the alginate microspheres.

As the coating composition is complex, with several layers of different components we will base the calculation on identifying characteristic processes of thermal degradation of the alginate core of the microspheres. In a TGA thermogram, all our samples show a rapid weight drop from the beginning of the scan due to water evaporation. It can be considered that when the heating scan reaches 200°C the sample is completely dry, and we use the weight measured at that temperature as the initial weight of the sample. Pure, uncoated alginate shows between 200 and 350°C a pronounced drop in weight due to thermal degradation that breaks chemical bonds in the chains and allows fragments of molecular size to evaporate (Figure 18_A). The process is more clearly seen if the derivative of weight respect to temperature is plotted so that the weight drop is shown as a peak. In calcium ion-crosslinked alginate, between 200 and 350°C two degradation peaks overlap as seen in Figure 18_B. Our results agree with the literature showing how the degradation of alginate in this temperature region depends on the presence of the ions used in the crosslinking [88].

The area under these two overlapping peaks measures the mass fraction of alginate lost between 200 and 350°C. To determine this precisely, a deconvolution of the thermogram in this

temperature interval has been performed, modeled with two Gaussians, one centered at 234°C and the other at 257°C. This yields a degraded alginate fraction of $w_{ALG} = 41\%$ of the weight of the dry sample.

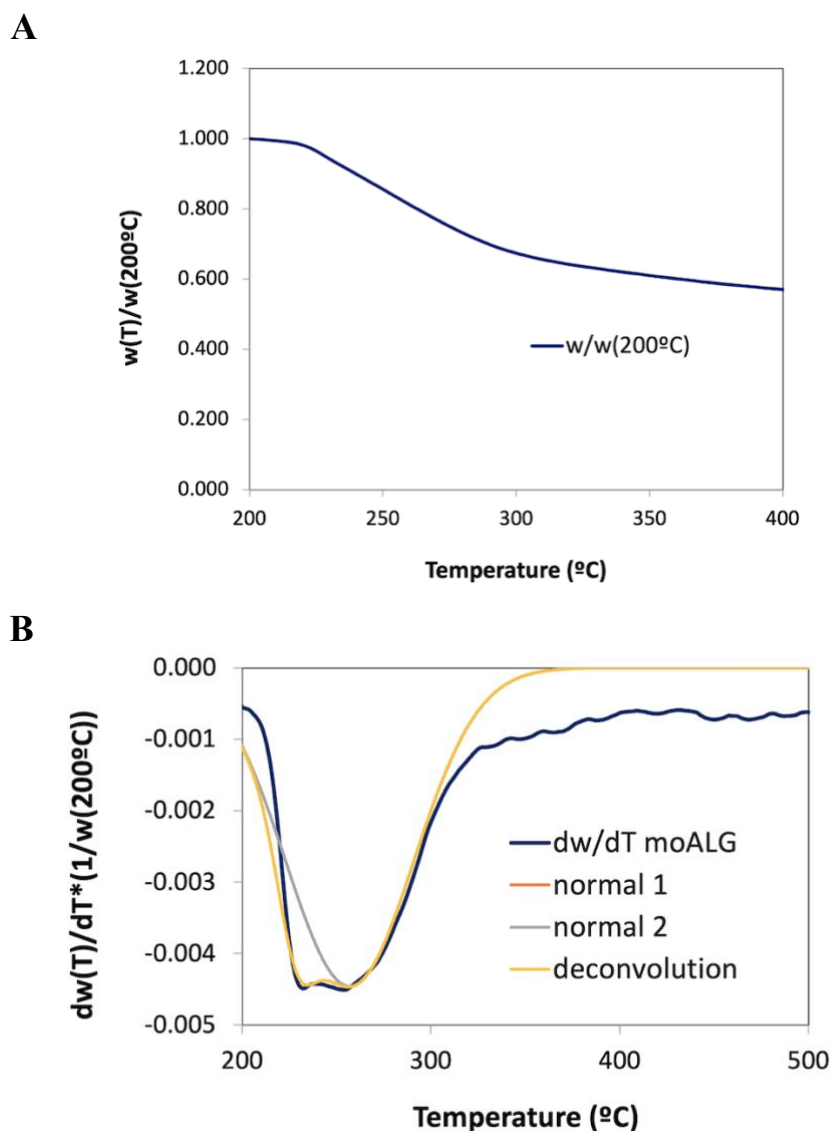


Figure 18. Sample weight (A) and temperature derivative (B) of alginate microspheres with reference to the dry weight of the sample.

In order to determine whether biomolecules are present on the microspheres' surface, we compared the curves of alginate microspheres with those functionalized using the LbL technique.

In Figure 19, the derivate reveals slight differences compared to the alginate graph. In fact, the two peaks are more distinctly separated from each other: one corresponds to 218°C, and the other to 264°C. Thus, showing that the interaction of the coating with the core of the microsphere and the possible delivering of calcium ions during coating formation can influence the degradation profile of the alginate network. Pure CS should have a thermal degradation

peak centered at 245°C (results not shown) so overlapping the range of the degradation of alginate we are considering. As stated above we cannot base the calculation on the area of this peak since the coating also contains other components, such as PLL and crosslinking agents. Thus, we calculate the area of the two peaks that we associate to alginate degradation that represent a $w_{\text{COAT}} = 37\%$ of the total mass of the sample. The ratio $w_{\text{COAT}}/w_{\text{ALG}} = 0.9$ allows us to deduce that 10% of the microsphere is coated with PLL/CS.

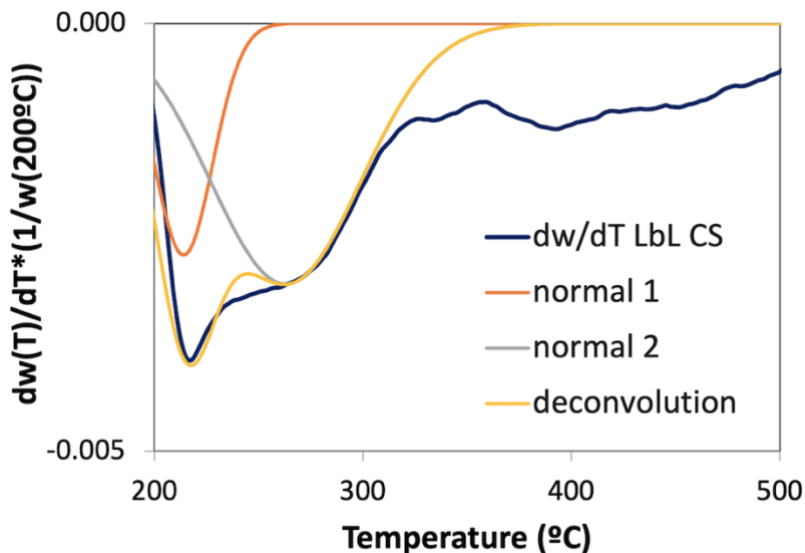


Figure 19. Derivative of the degradation of the dry weight of LbL PLL/CS microspheres.

The thermogram of the microspheres coated with LbL PLL/Hep is similar, as can be seen in Figure 20, which shows the derivate of the dry weight degradation. When compared to the alginate microspheres, the two peaks are both translated to the right, towards higher temperatures. The first peak is at 220°C, while the second one is centered at 272°C. The integration of the two peaks yields a fraction $W_{\text{COAT}} = 39\%$ of the total sample which means that the weight fraction of the coating is 5% in this case.

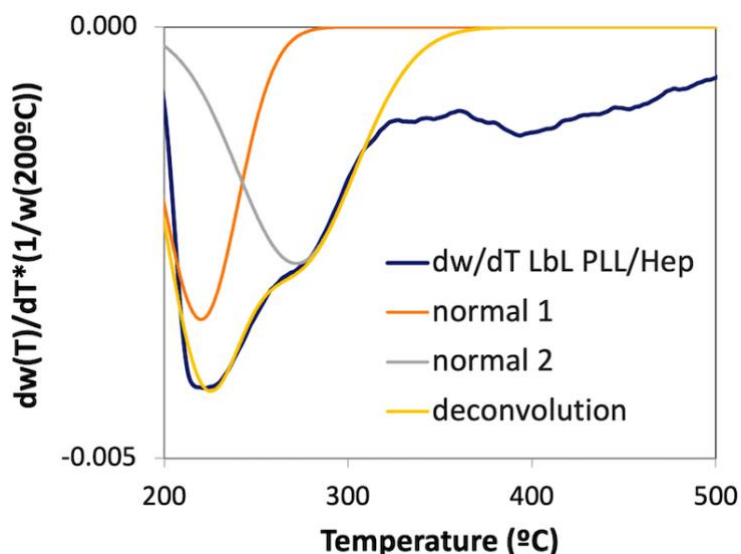


Figure 20. Derivative of the degradation of the dry weight of LbL PLL/Hep microspheres.

The deconvolution of the TGA curve of the microspheres coated with HA (Figure 21) needs the addition of a small peak at 206°C in addition to the two characteristic peaks of alginate degradation at 214 and 269°C respectively indicating the decomposition of more complex molecules, potentially associated with the breakdown of HA. The area of the alginate peaks is 37% of the total mass of the sample and thus, the fraction of the coating is 10% of the microsphere.

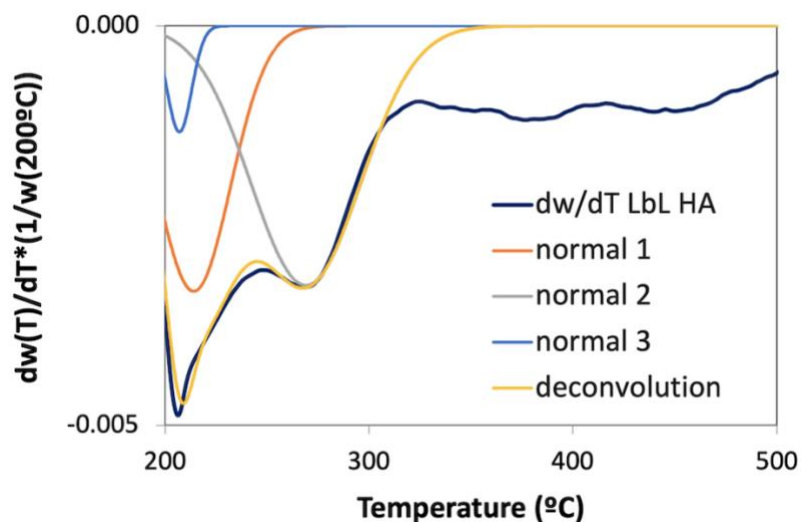
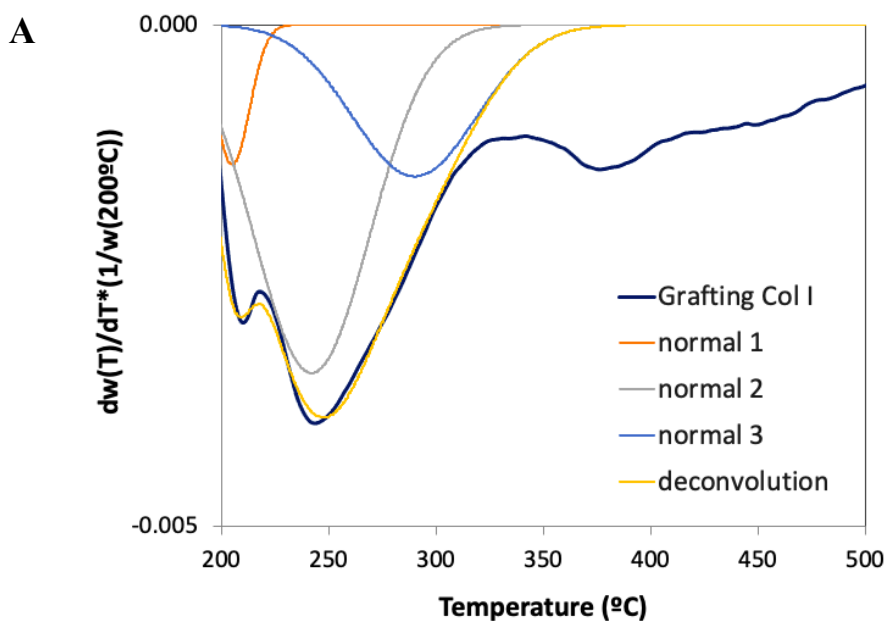


Figure 21. Derivative of the degradation of the dry weight of LbL PLL/HA microspheres.

Finally, Figure 22, illustrates the weight loss profile of microspheres coated with Col I. In this case, the thermogram is quite different from that of pure alginate, with a broad peak centered at 290°C that could have a significant contribution to the degradation of the grafted collagen since pure collagen type 1 presents its main degradation peak a 310°C. This prevents an accurate calculation of the mass fraction of collagen since the contribution of the degradation of alginate cannot be determined.



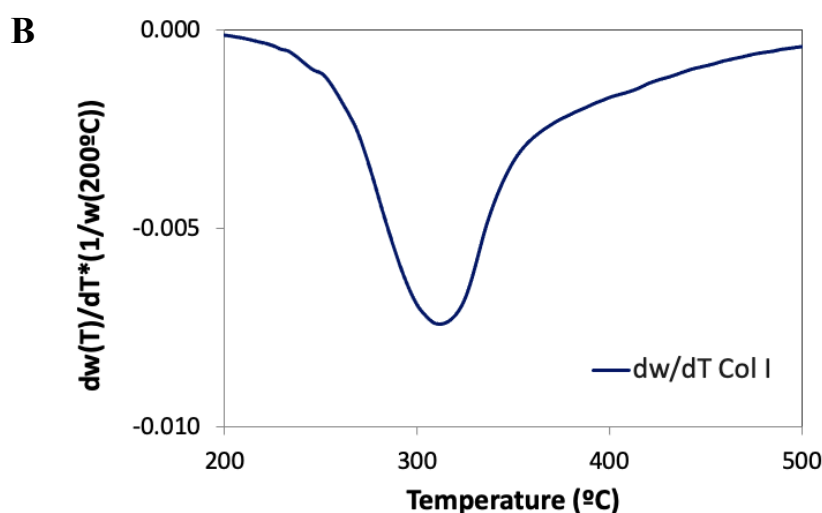


Figure 22. A) Derivative of the degradation of the dry weight of Col I grafted microspheres. B) Temperature derivative of the thermogram of pure collagen type I.

Comparing the TGA curves of microspheres with and without the coating, a noticeable shift in the onset temperature of decomposition is observed in the coated microspheres. This shift strongly implies that the presence of the LbL coating has a discernible impact on the thermal stability of the microspheres. The observed change in onset temperature suggests alterations in the thermal behavior induced by the LbL coating, indicating potential interactions and influences on the decomposition process.

4.3. Cell Culture

The cell cultures in this study are conducted under different conditions to test the hypotheses related to co-culture (direct and indirect) and culture with the microgel. The novelty introduced in this work is the cultivation in a static, yet 3D environment that promotes proliferation.

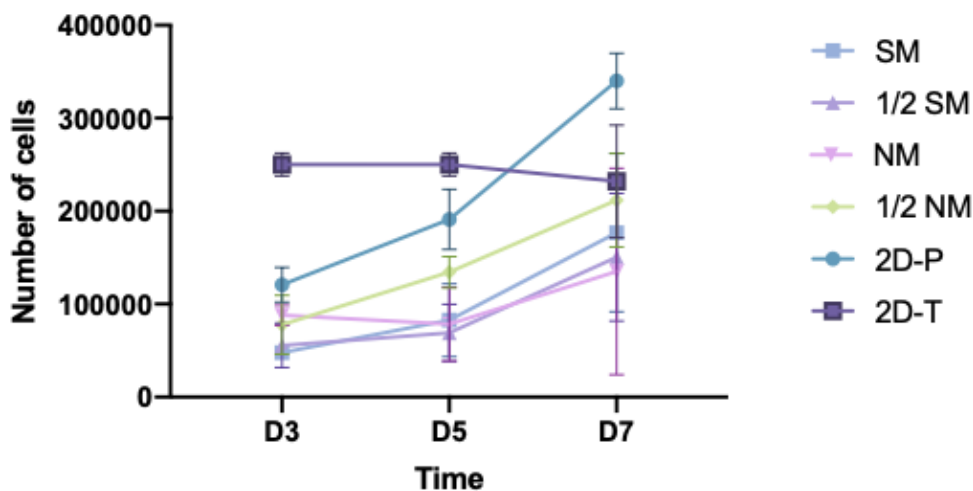
4.3.1. Culture to Set the Operating Conditions

MMCs were cultured on day 0 at a concentration of 60,000 cells / 100 μ L of culture medium under 2D conditions (Eppendorf tubes and p96 multiwell plate) and 3D conditions (hydrogels). In the case of 3D conditions, two different types of culture media were used: complete RPMI medium without phenol red (normal medium) and complete RPMI medium with a higher concentration of glucose (super medium). The culture medium was changed every two days in all conditions, but in the case of hydrogels, the medium change was done both completely and partially. Cell counting was performed on days 3, 5, and 7.

The assessment of cell proliferation in response to 2D and 3D conditions is a crucial aspect of cell culture research. The Neubauer chamber is a widely used tool in this regard, which enables cell counting. The present study employed the Neubauer chamber for cell counting to evaluate

the proliferation of cells under 2D and 3D conditions while accounting for the type and amount of the culture medium used. We call “normal medium” (NM) the complete RPMI culture medium and “super medium” (SM) the complete RPMI medium with a higher concentration of glucose. The results are presented in Figure 23.

a)



b)

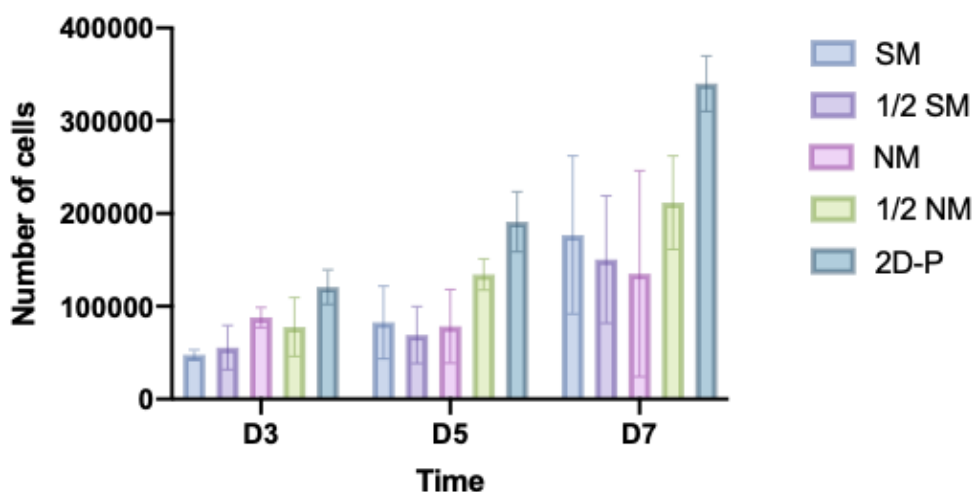


Figure 23. Number of cells at D3, D5, and D7. a) 2D and 3D conditions. b) 3D conditions with different types and amounts of medium change compared with the p96 condition.

In Figure 23_a) we can see how the 2D-T condition shows the highest number of cells at D3 between all conditions. However, the cell growth stops, to the extent that the number of cells does not increase between day 3 and day 5, and on day 7, it even decreases. For this reason, given that cells in the other conditions are actively proliferating, we opted not to consider this 2D condition.

As shown in Figure 23_b), the optimal 3D condition at day 3 is the complete change of normal medium but, despite that, during the 7 days of culture, the best results are provided by the partial

replacement of the normal medium. Conditions with the super medium do not provide better results.

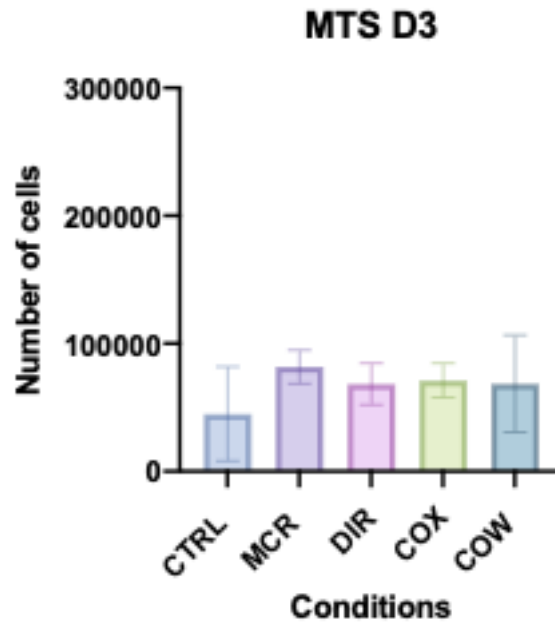
We found no significant differences between the different ways of renewing the culture medium in the conical agarose wells. Based on the mean values of cell numbers, we opted to proceed with a complete change of the normal medium for the cell cultures. This decision was driven by two main considerations. Firstly, while the half replacement of the normal medium yielded the best results over 7 days, the co-culture conditions have a cell number at least twice the number initially seeded in the culture protocol experiments. This indicates a heightened need for nutrients to support cell survival and proliferation. Secondly, given that the drug testing experiment (MTS) is conducted on day 3, and considering that the highest cell count is achieved with a complete change of the normal medium after 3 days of culture, this approach was deemed more suitable.

4.3.2. Cell Proliferation

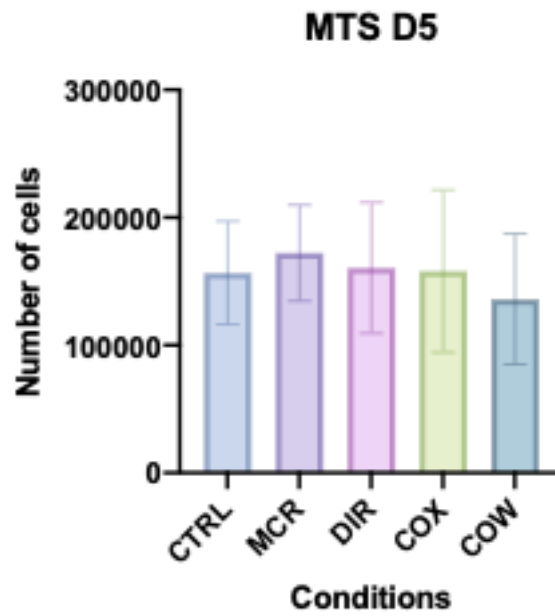
The cell culture is performed considering five different conditions. In addition to the control condition (CTRL) involving only MMCs and the one with MMCs and microgel (MCR), three co-culture conditions with hMSCs were implemented. In one instance, the hMSCs pellet is introduced inside the microwell (DIR condition). In contrast, in the remaining cases, the hMSCs pellet is positioned outside the agarose construct (COX and COW conditions). One of the indirect co-culture conditions (COW) also involves the microgel.

The following MTS assay was conducted on the MM1.S cell line to assess cellular proliferation under different culture conditions. The assay aims to provide information on cellular vitality and the potential effects of experimental conditions on cellular response.

A



B



C

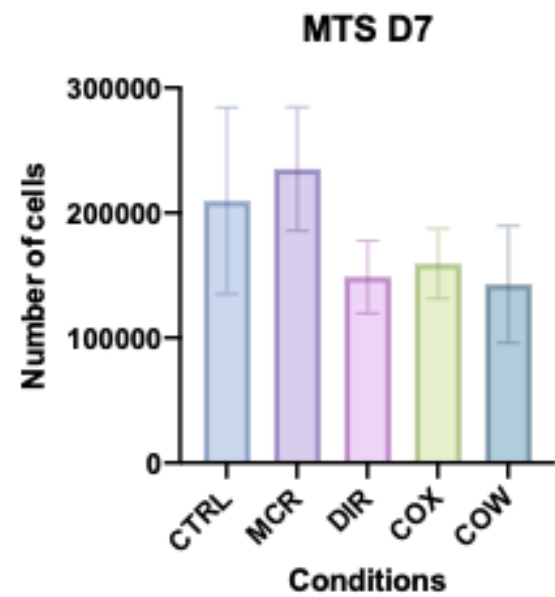


Figure 24. Proliferation MTS assay of MM1.S cells at day 3 (A), day 5 (B), and day 7 (C) under all conditions.

In Figure 24 we can see the number of cells at day 3, 5, and 7 under all conditions.

- CTRL: the number of cells in the control condition exhibits a gradual trend over time, indicating normal cell proliferation.
- MCR: cells in the culture condition with microspheres show a significant increase at 7 days, suggesting a potential positive effect of interaction with the microgels.
- DIR: the number of cells in direct co-culture increases from day 3 to day 5. Although soluble factor-mediated interaction favors proliferation, it has been observed that direct interaction between MMCs and hMSCs leads to the arrest of MMCs in non-proliferative phases of the cell cycle [89]. Nevertheless, between day 5 and day 7, the number of cells does not increase. This can be due to a lack of nutrients in the culture medium since the culture well contains both MMCs and MSCs.
- COX: the presence of the microgel appears to influence the proliferation dynamics, with a cellular response slightly different from other conditions but similar to direct co-culture. Looking at the graphs we can deduce that the microgels show a positive impact at day 3 and day 5, when the number of cells is higher than in the control, but proliferation stops, and the number of MMCs remains constant at day 7.
- COW: cell proliferation in the condition of indirect co-culture with microgels shows the poorest results, with a lower number of cells compared to other conditions.

Overall, it can be observed that, in almost all conditions, the number of cells increases as the days pass. The exception is the DIR condition, which seems to plateau after day 5, maintaining the same number of MMCs until day 7. Also, COX and COW conditions don't show a big increase in the number of cells between day 5 and day 7. Nevertheless, in no case, the number of cells is lower at day 5 and 7 than at day 3. This could indicate that what hindered the culture progression was not the saturation of the platform but the lack of nutrients for such a quantity of cells.

4.4. Drug Resistance

After demonstrating that the platform was appropriate for the three-dimensional culture of the MM1.S cell line, we assessed each condition's capacity to replicate resistance to MM drugs *in vitro*.

MM patients are currently treated clinically with dexamethasone (DEX) and bortezomib (BTZ). DEX is a glucocorticoid that causes MM cells apoptosis by activating intrinsic apoptotic pathways [90], cleaving poly (ADP-ribose) polymerase and caspase 3 [91], up-regulating pro-apoptotic genes, and down-regulating antiapoptotic genes [92].

To test the drug efficacy in our 3D platform, the MM1.S cell line was seeded and allowed to grow for 72 hours in two conditions: non-treated and DEX 1 μ M [75], [93]. Cell proliferation was measured with an MTS assay following a 72-hour culture.

In Figure 25 we can see how almost all conditions determine the generation of DEX resistance *in vitro*, except for the DIR condition. However, there are no significant statistical differences between treated and non-treated conditions.

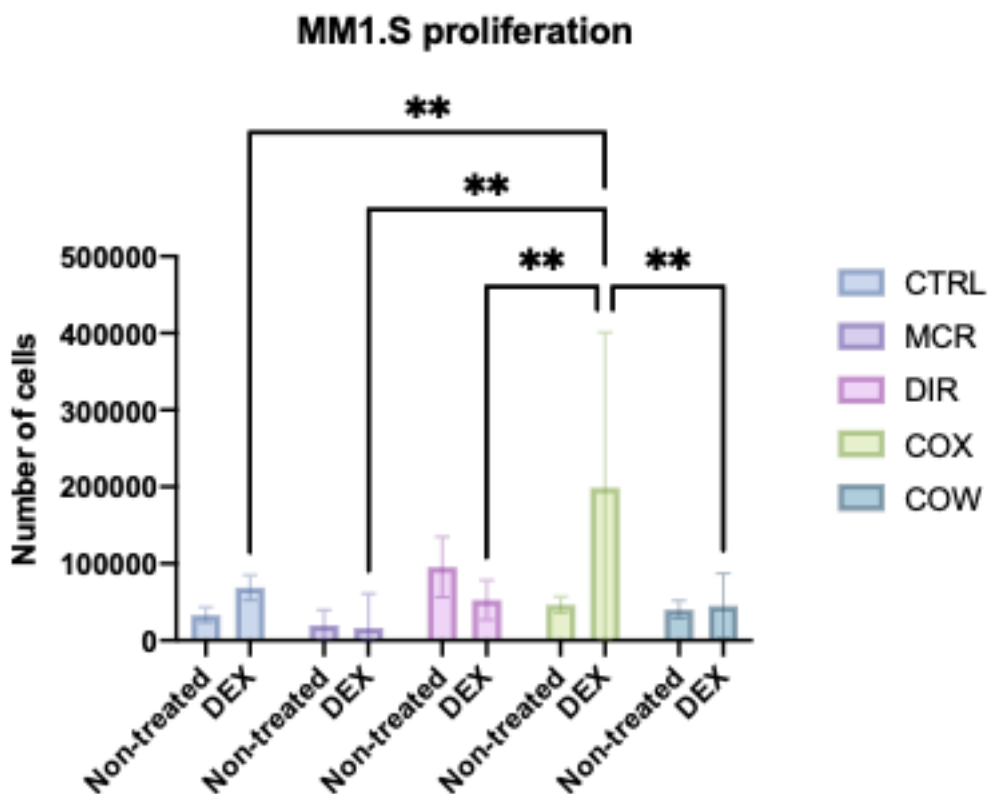


Figure 25. Proliferation rates of MM.1S cell line at 72 h of culture under all conditions treated with dexamethasone 1 μ M and non-treated conditions.

We found the cell behavior to be unusual and challenging to understand, possibly owing to the conical shape of the microwells that results in this peculiar DR. This phenomenon can be attributed to the fact that the cells exhibit limited growth beyond the third day of culture, as evidenced by the platform culture validation in section 4.3.2. Consequently, the drug's efficacy diminishes after this time point.

To confirm that our procedures were devoid of errors, we tested our platform with RPMI8226 cells that in preceding investigations showed a consistent response in dynamic 3D culture in different environments in which a suspension of the microspheres and the cells were maintained by an orbital agitation of the culture wells [53].

In the case of RPMI8226 cell line, we observed that MCR and COW conditions resulted in the highest resistance to DEX 1 μ M (as shown in Figure 26). This suggests that the microgel may have a crucial role in DR [42]. The resistance to DEX is more apparent in the static culture in the conical agarose wells in this work than in the mentioned references in the dynamic culture. Our findings are consistent with the literature on the effect of HA on CAM-DR. However, further research is required to understand the mechanism of DR on MM cells by CS, Hep, and Col I.

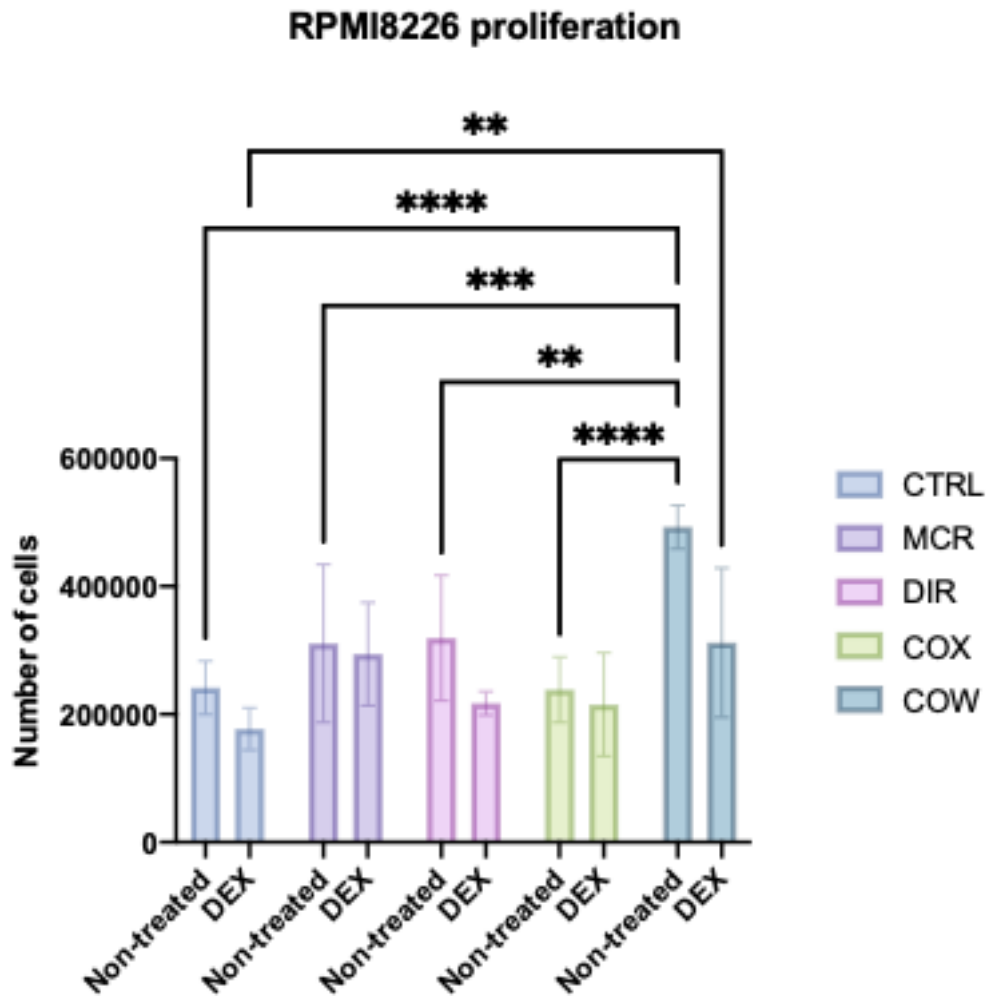


Figure 26. Proliferation rates of RPMI8226 cell line at 72 h of culture under all conditions treated with dexamethasone 1 μ M and non-treated conditions.

5. Conclusions

This Master thesis aimed to develop 3D culture environments that are specifically designed for the culture of multiple myeloma cells. These cells are known to be non-adherent and grow in suspension. Therefore, we explored the use of microspheres as a biomaterial. This approach is unique because it does not involve using microspheres as "cell-on" or "cell-in" supports for adherent cells. Instead, we developed the microgel concept, which entails a semi-solid culture medium where the microspheres and cells coexist in suspension without forcing the cells to adhere. The volume excluded by the microspheres in the culture well creates a 3D environment for the cells, bringing them closer together and increasing the effect of different interactions that may occur in the system, as opposed (or in contrast) to what would happen in a conventional 2D and suspension culture. These interactions can be either cell-cell, cell-microsphere, or cell-ECM, as the microspheres were designed to include components of the ECM. On that account, the findings of this work can be grouped into two main categories: first, the research focused on developing and analyzing biomaterials utilizing microspheres with specific properties, and second, the research aimed to integrate these materials into the myeloma cell culture to create a 3D platform.

The following conclusions can be highlighted:

- 1.5% w/w alginate microspheres with 5% w/WALG of ferrite nanoparticles have been obtained through microfluidics. The resultant microspheres have a narrow diameter distribution, which allows for proper size and shape. Additionally, the homogenous dispersion of the nanoparticles within the microspheres ensures uniformity.
- Alginate-based microspheres have been functionalized with biomolecules that are natural components of the BM ECM. The LbL method is an effective technique for functionalizing alginate microspheres, as it allows for the retention of polyelectrolytes that mimic the ECM. In fact, this method can be successfully used with three different pairs of polyelectrolytes. The effective incorporation of CS, Hep, and HA on the surface of the microspheres has been demonstrated.
- Collagen can be grafted onto the PLL-functionalized surface of alginate microspheres using glutaraldehyde covalent crosslinking. The pre-coating and the protocol could be modified to achieve a higher degree of collagen grafting onto the surface.
- The complete RPMI culture medium with 2 g/L of glucose has proven to be the best choice for MM1.S cell line culture, compared to the medium with a higher amount of glucose (4.5 g/L).

- The potential of the microgel platform as an *in vitro* model for MM has been demonstrated, as it has a positive effect on cell viability and proliferation and seems to be crucial in MM cell culture.
- The 3D culture platform allows the interaction between mPCs and ECM components on the surface of the microspheres.
- Indirect co-culture is the chosen approach for further assays as it is simpler to handle and appears to have better effects on MM cells, giving better results compared to the direct condition which shows the lowest cell proliferation.
- The effect of microgel in the generation of DR effect to DEX in RPMI8226 cell line has been verified. The study's results align with the current understanding of the effect of HA on CAM-DR. Nevertheless, the exact mechanism of drug resistance on MM cells by CS, Hep, and Col I remains to be fully understood. Further studies are necessary to shed light on the intricate details of this process and pave the way for more effective treatments.
- This research work presents a wide number of research opportunities for further exploration. One such area of interest is the development of 3D cultures that integrate different ECM components as well as the co-culture with hMSCs. Another promising area of research is the validation of this platform for the culture of primary cells taken from patients with MM which, once validated, could be applied for the testing and development of new drugs. This could lead to a better understanding of their effects as well as the interaction between neoplastic cells and the bone marrow microenvironment.

Bibliography

- [1] G. S. Travlos, "Normal Structure, Function, and Histology of the Bone Marrow," *Toxicol Pathol*, vol. 34, no. 5, 2006, doi: 10.1080/01926230600939856.
- [2] D. Lucas, "Structural organization of the bone marrow and its role in hematopoiesis," *Current Opinion in Hematology*, vol. 28, no. 1. 2021. doi: 10.1097/MOH.0000000000000621.
- [3] M. Galán-Diez, Á. Cuesta-Domínguez, and S. Kousteni, "The bone marrow microenvironment in health and myeloid malignancy," *Cold Spring Harb Perspect Med*, vol. 8, no. 7, 2018, doi: 10.1101/cshperspect.a031328.
- [4] A. A. Wang, J. L. Gommerman, and O. L. Rojas, "Plasma Cells: From Cytokine Production to Regulation in Experimental Autoimmune Encephalomyelitis," *Journal of Molecular Biology*, vol. 433, no. 1. 2021. doi: 10.1016/j.jmb.2020.09.014.
- [5] J. Banchereau and F. Rousset, "Human B lymphocytes: Phenotype, proliferation, and differentiation," *Adv Immunol*, vol. 52, 1992, doi: 10.1016/s0065-2776(08)60876-7.
- [6] P. D. Pioli, "Plasma Cells, the Next Generation: Beyond Antibody Secretion," *Front Immunol*, vol. 10, 2019, doi: 10.3389/fimmu.2019.02768.
- [7] H. C. Allen and P. Sharma, *Histology, Plasma Cells*. 2020.
- [8] R. Hoffman and B. K. Marcellino, "Bone Marrow Microenvironment in Health and Disease," in *Encyclopedia of Bone Biology*, Elsevier, 2020, pp. 1–11. doi: 10.1016/B978-0-12-801238-3.11195-X.
- [9] D. Verma and D. S. Krause, "Targeting the Bone Marrow Niche in Hematological Malignancies," 2017, pp. 155–175. doi: 10.1016/bs.asn.2016.12.004.
- [10] S. Méndez-Ferrer *et al.*, "Bone marrow niches in haematological malignancies," *Nature Reviews Cancer*, vol. 20, no. 5. 2020. doi: 10.1038/s41568-020-0245-2.
- [11] Y. Shiozawa, "The Roles of Bone Marrow-Resident Cells as a Microenvironment for Bone Metastasis," in *Advances in Experimental Medicine and Biology*, vol. 1226, 2020. doi: 10.1007/978-3-030-36214-0_5.
- [12] R. Florencio-Silva, G. R. D. S. Sasso, E. Sasso-Cerri, M. J. Simões, and P. S. Cerri, "Biology of Bone Tissue: Structure, Function, and Factors That Influence Bone Cells," *BioMed Research International*, vol. 2015. 2015. doi: 10.1155/2015/421746.
- [13] M. C. Horowitz *et al.*, "Bone marrow adipocytes," *Adipocyte*, vol. 6, no. 3. 2017. doi: 10.1080/21623945.2017.1367881.
- [14] T. Itkin *et al.*, "Distinct bone marrow blood vessels differentially regulate haematopoiesis," *Nature*, vol. 532, no. 7599, 2016, doi: 10.1038/nature17624.
- [15] O. Kandarakov, A. Belyavsky, and E. Semenova, "Bone Marrow Niches of Hematopoietic Stem and Progenitor Cells," *International Journal of Molecular Sciences*, vol. 23, no. 8. 2022. doi: 10.3390/ijms23084462.
- [16] T. Morikawa and K. Takubo, "Use of imaging techniques to illuminate dynamics of hematopoietic stem cells and their niches," *Frontiers in Cell and Developmental Biology*, vol. 5, no. JUN. 2017. doi: 10.3389/fcell.2017.00062.
- [17] D. C. Ding, W. C. Shyu, and S. Z. Lin, "Mesenchymal stem cells," *Cell Transplantation*, vol. 20, no. 1. 2011. doi: 10.3727/096368910X.
- [18] M. R. Reagan and I. M. Ghobrial, "Multiple myeloma mesenchymal stem cells: Characterization, origin, and tumor-promoting effects," *Clinical Cancer Research*, vol. 18, no. 2. 2012. doi: 10.1158/1078-0432.CCR-11-2212.
- [19] K. Brigle and B. Rogers, "Pathobiology and Diagnosis of Multiple Myeloma," *Seminars in Oncology Nursing*, vol. 33, no. 3. 2017. doi: 10.1016/j.soncn.2017.05.012.
- [20] R. Kumar, P. S. Godavarthy, and D. S. Krause, "The bone marrow microenvironment in health and disease at a glance," *J Cell Sci*, vol. 131, no. 4, 2018, doi: 10.1242/jcs.201707.

- [21] S. Klamer and C. Voermans, "The role of novel and known extracellular matrix and adhesion molecules in the homeostatic and regenerative bone marrow microenvironment <http://www.tandfonline.com/doi/pdf/10.4161/19336918.2014.968501>," *Cell Adhesion and Migration*, vol. 8, no. 6. 2014. doi: 10.4161/19336918.2014.968501.
- [22] M. J. Domingues, H. Cao, S. Y. Heazlewood, B. Cao, and S. K. Nilsson, "Niche Extracellular Matrix Components and Their Influence on HSC," *J Cell Biochem*, vol. 118, no. 8, 2017, doi: 10.1002/jcb.25905.
- [23] R. A. Kyle and S. V. Rajkumar, "Multiple myeloma," *Blood*, vol. 111, no. 6. 2008. doi: 10.1182/blood-2007-10-078022.
- [24] C. S. Mitsiades, N. Mitsiades, N. C. Munshi, and K. C. Anderson, "Focus on multiple myeloma," *Cancer Cell*, vol. 6, no. 5. 2004. doi: 10.1016/j.ccr.2004.10.020.
- [25] S. Kassem *et al.*, "SAR442085, a novel anti-CD38 antibody with enhanced antitumor activity against multiple myeloma," *Blood*, vol. 139, no. 8, 2022, doi: 10.1182/blood.2021012448.
- [26] A. J. Cowan *et al.*, "Diagnosis and Management of Multiple Myeloma: A Review," *JAMA*, vol. 327, no. 5. 2022. doi: 10.1001/jama.2022.0003.
- [27] S. M. Prideaux, E. Conway O'Brien, and T. J. Chevassut, "The genetic architecture of multiple myeloma," *Advances in Hematology*, vol. 2014. 2014. doi: 10.1155/2014/864058.
- [28] J. G. Lohr *et al.*, "Widespread genetic heterogeneity in multiple myeloma: Implications for targeted therapy," *Cancer Cell*, vol. 25, no. 1, 2014, doi: 10.1016/j.ccr.2013.12.015.
- [29] H. E. Johnsen *et al.*, "The myeloma stem cell concept, revisited: From phenomenology to operational terms," *Haematologica*, vol. 101, no. 12. 2016. doi: 10.3324/haematol.2015.138826.
- [30] S. A. Minnie and G. R. Hill, "Immunotherapy of multiple myeloma," *Journal of Clinical Investigation*, vol. 130, no. 4, 2020, doi: 10.1172/JCI129205.
- [31] C. Y. Soekjojo and W. J. Chng, "Treatment horizon in multiple myeloma," *European Journal of Haematology*, vol. 109, no. 5. 2022. doi: 10.1111/ejh.13840.
- [32] V. Pinto, R. Bergantim, H. R. Caires, H. Seca, J. E. Guimarães, and M. H. Vasconcelos, "Multiple myeloma: Available therapies and causes of drug resistance," *Cancers*, vol. 12, no. 2. 2020. doi: 10.3390/cancers12020407.
- [33] C. S. Chim *et al.*, "Management of relapsed and refractory multiple myeloma: Novel agents, antibodies, immunotherapies and beyond," *Leukemia*, vol. 32, no. 2. 2018. doi: 10.1038/leu.2017.329.
- [34] C. Kervoëlen *et al.*, "Dexamethasone-induced cell death is restricted to specific molecular subgroups of multiple myeloma," *Oncotarget*, vol. 6, no. 29, 2015, doi: 10.18632/oncotarget.4616.
- [35] P. Robak, I. Drozd, J. Szemraj, and T. Robak, "Drug resistance in multiple myeloma," *Cancer Treatment Reviews*, vol. 70. 2018. doi: 10.1016/j.ctrv.2018.09.001.
- [36] T. Vincent and N. Mehti, "Extracellular matrix in bone marrow can mediate drug resistance in myeloma," *Leukemia and Lymphoma*, vol. 46, no. 6. 2005. doi: 10.1080/10428190500051448.
- [37] J. Corre *et al.*, "Bone marrow mesenchymal stem cells are abnormal in multiple myeloma," *Leukemia*, vol. 21, no. 5, 2007, doi: 10.1038/sj.leu.2404621.
- [38] U. Yanamandra and S. K. Kumar, "Minimal residual disease analysis in myeloma—when, why and where," *Leukemia and Lymphoma*, vol. 59, no. 8. 2018. doi: 10.1080/10428194.2017.1386304.
- [39] L. A. Hazlehurst and W. S. Dalton, "De Novo and Acquired Resistance to Antitumor Alkylating Agents," in *Cancer Drug Resistance*, 2007. doi: 10.1007/978-1-59745-035-5_20.

- [40] M. B. Meads, L. A. Hazlehurst, and W. S. Dalton, "The bone marrow microenvironment as a tumor sanctuary and contributor to drug resistance," *Clinical Cancer Research*, vol. 14, no. 9, 2008, doi: 10.1158/1078-0432.CCR-07-2223.
- [41] N. Volpi, J. Schiller, R. Stern, and L. Soltés, "Role, Metabolism, Chemical Modifications and Applications of Hyaluronan," *Curr Med Chem*, vol. 16, no. 14, 2009, doi: 10.2174/092986709788186138.
- [42] T. Vincent, L. Molina, L. Espert, and N. Mechti, "Hyaluronan, a major non-protein glycosaminoglycan component of the extracellular matrix in human bone marrow, mediates dexamethasone resistance in multiple myeloma," *Br J Haematol*, vol. 121, no. 2, pp. 259–269, Apr. 2003, doi: 10.1046/j.1365-2141.2003.04282.x.
- [43] T. Vincent, M. Jourdan, M. S. Sy, B. Klein, and N. Mechti, "Hyaluronic Acid Induces Survival and Proliferation of Human Myeloma Cells through an Interleukin-6-mediated Pathway Involving the Phosphorylation of Retinoblastoma Protein," *Journal of Biological Chemistry*, vol. 276, no. 18, 2001, doi: 10.1074/jbc.M003965200.
- [44] C. C. Bjorklund *et al.*, "Evidence of a role for CD44 and cell adhesion in mediating resistance to lenalidomide in multiple myeloma: Therapeutic implications," *Leukemia*, vol. 28, no. 2, 2014, doi: 10.1038/leu.2013.174.
- [45] T. Mikami and H. Kitagawa, "Biosynthesis and function of chondroitin sulfate," *Biochimica et Biophysica Acta - General Subjects*, vol. 1830, no. 10, 2013. doi: 10.1016/j.bbagen.2013.06.006.
- [46] N. S. Gandhi and R. L. Mancera, "The structure of glycosaminoglycans and their interactions with proteins," *Chemical Biology and Drug Design*, vol. 72, no. 6, 2008. doi: 10.1111/j.1747-0285.2008.00741.x.
- [47] T. Mikami and H. Kitagawa, "Chondroitin sulfate glycosaminoglycans function as extra/pericellular ligands for cell surface receptors," *Journal of Biochemistry*, vol. 173, no. 5, 2023. doi: 10.1093/jb/mvac110.
- [48] V. Gauba and J. D. Hartgerink, "Self-assembled heterotrimeric collagen triple helices directed through electrostatic interactions," *J Am Chem Soc*, vol. 129, no. 9, 2007, doi: 10.1021/ja0683640.
- [49] N. I. Nissen, M. Karsdal, and N. Willumsen, "Collagens and Cancer associated fibroblasts in the reactive stroma and its relation to Cancer biology," *Journal of Experimental and Clinical Cancer Research*, vol. 38, no. 1, 2019. doi: 10.1186/s13046-019-1110-6.
- [50] N. S. Lewis, E. E. L. Lewis, M. Mullin, H. Wheadon, M. J. Dalby, and C. C. Berry, "Magnetically levitated mesenchymal stem cell spheroids cultured with a collagen gel maintain phenotype and quiescence," *J Tissue Eng*, vol. 8, 2017, doi: 10.1177/2041731417704428.
- [51] R. Ridley, H. Xiao, H. Hata, J. Woodliff, J. Epstein, and R. Sanderson, "Expression of syndecan regulates human myeloma plasma cell adhesion to type I collagen," *Blood*, vol. 81, no. 3, pp. 767–774, Feb. 1993, doi: 10.1182/blood.V81.3.767.767.
- [52] Z. Ren *et al.*, "Syndecan-1 promotes Wnt/ β -catenin signaling in multiple myeloma by presenting Wnts and R-spondins," *Blood*, vol. 131, no. 9, pp. 982–994, Mar. 2018, doi: 10.1182/blood-2017-07-797050.
- [53] J. C. Marín-Payá *et al.*, "Biomimetic 3d environment based on microgels as a model for the generation of drug resistance in multiple myeloma," *Materials*, vol. 14, no. 23, 2021, doi: 10.3390/ma14237121.
- [54] A. Casu, "Heparin structure," *Pathophysiol Haemost Thromb*, vol. 20, 1990, doi: 10.1159/000216162.
- [55] J. Atallah, H. H. Khachfe, J. Berro, and H. I. Assi, "The use of heparin and heparin-like molecules in cancer treatment: a review," *Cancer Treatment and Research Communications*, vol. 24, 2020. doi: 10.1016/j.ctarc.2020.100192.

- [56] R. D. Sanderson and Y. Yang, "Syndecan-1: A dynamic regulator of the myeloma microenvironment," *Clinical and Experimental Metastasis*, vol. 25, no. 2. 2008. doi: 10.1007/s10585-007-9125-3.
- [57] K. C. Anderson *et al.*, "Multiple Myeloma: New Insights and Therapeutic Approaches," *Hematology*, vol. 2000, no. 1, 2000, doi: 10.1182/asheducation.v2000.1.147.20000147.
- [58] R. Edmondson, J. J. Broglie, A. F. Adcock, and L. Yang, "Three-dimensional cell culture systems and their applications in drug discovery and cell-based biosensors," *Assay and Drug Development Technologies*, vol. 12, no. 4. 2014. doi: 10.1089/adt.2014.573.
- [59] D. Lourenço, R. Lopes, C. Pestana, A. C. Queirós, C. João, and E. A. Carneiro, "Patient-Derived Multiple Myeloma 3D Models for Personalized Medicine—Are We There Yet?," *International Journal of Molecular Sciences*, vol. 23, no. 21. 2022. doi: 10.3390/ijms232112888.
- [60] F. Pampaloni, E. G. Reynaud, and E. H. K. Stelzer, "The third dimension bridges the gap between cell culture and live tissue," *Nature Reviews Molecular Cell Biology*, vol. 8, no. 10. 2007. doi: 10.1038/nrm2236.
- [61] D. Belloni *et al.*, "Modeling multiple myeloma-bone marrow interactions and response to drugs in a 3d surrogate microenvironment," *Haematologica*, vol. 103, no. 4, 2018, doi: 10.3324/haematol.2017.167486.
- [62] N. Chaicharoenaudomrung, P. Kunhorm, and P. Noisa, "Three-dimensional cell culture systems as an *in vitro* platform for cancer and stem cell modeling," *World Journal of Stem Cells*, vol. 11, no. 12. 2019. doi: 10.4252/wjsc.v11.i12.1065.
- [63] L. Huang, A. M. E. Abdalla, L. Xiao, and G. Yang, "Biopolymer-based microcarriers for three-dimensional cell culture and engineered tissue formation," *International Journal of Molecular Sciences*, vol. 21, no. 5. 2020. doi: 10.3390/ijms21051895.
- [64] C. Humpel, "Organotypic brain slice cultures: A review," *Neuroscience*, vol. 305, 2015, doi: 10.1016/j.neuroscience.2015.07.086.
- [65] G. Mehta, A. Y. Hsiao, M. Ingram, G. D. Luker, and S. Takayama, "Opportunities and challenges for use of tumor spheroids as models to test drug delivery and efficacy," *Journal of Controlled Release*, vol. 164, no. 2, 2012, doi: 10.1016/j.jconrel.2012.04.045.
- [66] D. Khaitan, S. Chandna, M. B. Arya, and B. S. Dwarakanath, "Establishment and characterization of multicellular spheroids from a human glioma cell line; implications for tumor therapy," *J Transl Med*, vol. 4, 2006, doi: 10.1186/1479-5876-4-12.
- [67] J. L. Drury and D. J. Mooney, "Hydrogels for tissue engineering: Scaffold design variables and applications," *Biomaterials*, vol. 24, no. 24. 2003. doi: 10.1016/S0142-9612(03)00340-5.
- [68] R. Alfred *et al.*, "Efficient suspension bioreactor expansion of murine embryonic stem cells on microcarriers in serum-free medium," *Biotechnol Prog*, vol. 27, no. 3, 2011, doi: 10.1002/btpr.591.
- [69] S. Derakhti, S. H. Safiabadi-Tali, G. Amoabediny, and M. Sheikhpour, "Attachment and detachment strategies in microcarrier-based cell culture technology: A comprehensive review," *Materials Science and Engineering C*, vol. 103. 2019. doi: 10.1016/j.msec.2019.109782.
- [70] A. S. Caldwell, B. A. Aguado, and K. S. Anseth, "Designing Microgels for Cell Culture and Controlled Assembly of Tissue Microenvironments," *Advanced Functional Materials*, vol. 30, no. 37. 2020. doi: 10.1002/adfm.201907670.
- [71] J. P. Newsom, K. A. Payne, and M. D. Krebs, "Microgels: Modular, tunable constructs for tissue regeneration," *Acta Biomaterialia*, vol. 88. 2019. doi: 10.1016/j.actbio.2019.02.011.

- [72] T. Andersen, P. Auk-Emblem, and M. Dornish, "3D Cell Culture in Alginate Hydrogels," *Microarrays*, vol. 4, no. 2, 2015, doi: 10.3390/microarrays4020133.
- [73] D. R. Sahoo and T. Biswal, "Alginate and its application to tissue engineering," *SN Applied Sciences*, vol. 3, no. 1, 2021. doi: 10.1007/s42452-020-04096-w.
- [74] M. Ferrarini, M. Marcatti, F. Ciceri, and E. Ferrero, "3D Models of Surrogate Multiple Myeloma Bone Marrow Microenvironments: Insights on Disease Pathophysiology and Patient-Specific Response to Drugs," in *Multiple Myeloma*, 2021. doi: 10.5772/intechopen.95333.
- [75] J. Jakubikova *et al.*, "A novel 3D mesenchymal stem cell model of the multiple myeloma bone marrow niche: Biologic and clinical applications," *Oncotarget*, vol. 7, no. 47, 2016, doi: 10.18632/oncotarget.12643.
- [76] J. Kirshner *et al.*, "A unique three-dimensional model for evaluating the impact of therapy on multiple myeloma," *Blood*, vol. 112, no. 7, 2008, doi: 10.1182/blood-2008-02-142430.
- [77] P. de la Puente *et al.*, "3D tissue-engineered bone marrow as a novel model to study pathophysiology and drug resistance in multiple myeloma," *Biomaterials*, vol. 73, 2015, doi: 10.1016/j.biomaterials.2015.09.017.
- [78] M. Ferrarini *et al.*, "Ex-Vivo Dynamic 3-D Culture of Human Tissues in the RCCSTM Bioreactor Allows the Study of Multiple Myeloma Biology and Response to Therapy," *PLoS One*, vol. 8, no. 8, 2013, doi: 10.1371/journal.pone.0071613.
- [79] G. Mazzoleni, F. Boukhechba, N. Steimberg, J. Boniotti, J. M. Bouler, and N. Rochet, "Impact of dynamic culture in the RCCSTM bioreactor on a three-dimensional model of bone matrix formation," in *Procedia Engineering*, 2011. doi: 10.1016/j.proeng.2011.04.603.
- [80] J. L. Becker and G. R. Souza, "Using space-based investigations to inform cancer research on Earth," *Nature Reviews Cancer*, vol. 13, no. 5, 2013. doi: 10.1038/nrc3507.
- [81] J. C. Marín-Payá, S. Clara-Trujillo, L. Cordón, G. Gallego Ferrer, A. Sempere, and J. L. Gómez Ribelles, "Protein-Functionalized Microgel for Multiple Myeloma Cells' 3D Culture," *Biomedicines*, vol. 10, no. 11, 2022, doi: 10.3390/biomedicines10112797.
- [82] S. Clara-Trujillo, L. Tolosa, L. Cordón, A. Sempere, G. Gallego Ferrer, and J. L. Gómez Ribelles, "Novel microgel culture system as semi-solid three-dimensional *in vitro* model for the study of multiple myeloma proliferation and drug resistance," *Biomaterials Advances*, vol. 135, 2022, doi: 10.1016/j.bioadv.2022.212749.
- [83] M. Kamali and A. Ghahremaninezhad, "A study of calcium-silicate-hydrate/polymer nanocomposites fabricated using the layer-by-layer method," *Materials*, vol. 11, no. 4, 2018, doi: 10.3390/ma11040527.
- [84] D. Giannakoudakis, L. Meili, and I. Anastopoulos, *Novel Materials for Environmental Remediation Applications: Adsorption and Beyond*. 2022. doi: 10.1016/B978-0-323-91894-7.09992-8.
- [85] K. R. Rajisha, B. Deepa, L. A. Pothan, and S. Thomas, "Thermomechanical and spectroscopic characterization of natural fibre composites," in *Interface Engineering of Natural Fibre Composites for Maximum Performance*, 2011. doi: 10.1016/B978-1-84569-742-6.50009-5.
- [86] A. R. Thomsen *et al.*, "A deep conical agarose microwell array for adhesion independent three-dimensional cell culture and dynamic volume measurement," *Lab Chip*, vol. 18, no. 1, 2018, doi: 10.1039/c7lc00832e.
- [87] Š. Selimović, F. Piraino, H. Bae, M. Rasponi, A. Redaelli, and A. Khademhosseini, "Microfabricated polyester conical microwells for cell culture applications," *Lab Chip*, vol. 11, no. 14, 2011, doi: 10.1039/c1lc20213h.
- [88] M. I. García-Briega *et al.*, "Stability of Biomimetically Functionalised Alginate Microspheres as 3D Support in Cell Cultures," *Polymers (Basel)*, vol. 14, no. 20, 2022, doi: 10.3390/polym14204282.

- [89] Y. Nefedova, T. H. Landowski, and W. S. Dalton, "Bone marrow stromal-derived soluble factors and direct cell contact contribute to de novo drug resistance of myeloma cells by distinct mechanisms," *Leukemia*, vol. 17, no. 6, 2003, doi: 10.1038/sj.leu.2402924.
- [90] D. Chauhan, T. Hideshima, S. Rosen, J. C. Reed, S. Kharbanda, and K. C. Anderson, "Apaf-1/Cytochrome c-independent and Smac-dependent Induction of Apoptosis in Multiple Myeloma (MM) Cells," *Journal of Biological Chemistry*, vol. 276, no. 27, pp. 24453–24456, Jan. 2001, doi: 10.1074/jbc.C100074200.
- [91] D. Chauhan *et al.*, "Dexamethasone induces apoptosis of multiple myeloma cells in a JNK/SAP kinase independent mechanism," *Oncogene*, vol. 15, no. 7, 1997, doi: 10.1038/sj.onc.1201253.
- [92] N. Burwick and S. Sharma, "Glucocorticoids in multiple myeloma: past, present, and future," *Annals of Hematology*, vol. 98, no. 1. 2019. doi: 10.1007/s00277-018-3465-8.
- [93] C. Ohwada *et al.*, "CD44 and hyaluronan engagement promotes dexamethasone resistance in human myeloma cells," *Eur J Haematol*, vol. 80, no. 3, 2008, doi: 10.1111/j.1600-0609.2007.01014.x.